DTIC FILE COPY

National Defence
Research and
Development Branch

Défense Nationale
Bureau de Recherche
et Développment

AD-A189 434

REPORT 87/101
July 1987

ESTIMATION OF AZIMUTHAL AND VERTICAL ARRIVAL ANGLES AT A ROTATABLE HORIZONTAL LINE ARRAY

B.A. Trenholm — James A. Theriault

**Defence
Research
Establishment
Atlantic**

**Centre de
Recherches pour la
Défense
Atlantique**

DTIC
ELECTE
DEC 1 0 1987
S E D

Canada

8 7 11 30 036

DEFENCE RESEARCH ESTABLISHMENT ATLANTIC

9 GROVE STREET	P.O. BOX 1012	
	DARTMOUTH, N.S.	TELEPHONE
	B2Y 3Z7	(902) 426.3100

CENTRE DE RECHERCHES POUR LA DÉFENSE ATLANTIQUE

9 GROVE STREET	C.P. 1012
	DARTMOUTH, N.É.
	B2Y 3Z7

I✦ National Defence   Défense Nationale
Research and   Bureau de Recherche
Development Branch   et Développment

ESTIMATION OF AZIMUTHAL AND VERTICAL ARRIVAL ANGLES AT A ROTATABLE HORIZONTAL LINE ARRAY

B.A. Trenholm – James A. Theriault

July 1987

Approved by R.F. Brown   Director/Underwater Acoustics Division

DISTRIBUTION APPROVED BY

CHIEF D.R.E.A.

REPORT 87/101

Defence   Centre de
Research   Recherches pour la
Establishment   Défense
Atlantic   Atlantique

Canada

ABSTRACT

A Horizontal Line Array (HLA) receiver is subject to left-right bearing ambiguity. It is also susceptible to bearing bias caused by non-zero vertical arrival angles. The true bearing angle and the vertical arrival angle may both be estimated if a second observation is made, with the HLA rotated to a new orientation. A closed-form solution is presented for the case of stationary source and receiver. For small observation errors, the resulting errors in the estimated angles can also be expressed in closed form.

RÉSUMÉ

Les récepteurs de sonar en ligne horizontale (Horizontal Line Array, HLA) sont sujets à des ambiguités à gauche ou à droite quant au relèvement. Ils sont également sujets à des erreurs de relèvement causées par des angles d'arrivée non nuls par rapport à la verticale. Le relèvement véritable et l'angle d'arrivée par rapport à la verticale peuvent tous deux être estimés si on effectue une deuxième observation après avoir aligné le HLA sur un nouveau cap. Une solution analytique complète est présentée pour le cas d'une source et d'un récepteur stationnaires. Pour de petites erreurs d'observation, les erreurs résultantes des angles estimés peuvent également être exprimées sous forme de solution analytique complète.

Contents

1 Introduction

A Horizontal Line Array (HLA) receiver is a one-dimensional array of sensors lying in the horizontal plane. An HLA can be used to detect an underwater acoustic source, and to obtain an estimate of the direction of the arriving signal. Due to the one-dimensional nature of the HLA, the bearing estimates are subject to left-right ambiguity. HLA bearing estimates are also susceptible to bearing bias caused by non-zero vertical arrival angles.

The true bearing angle and the vertical arrival angle may both be estimated if a second observation is made. This can be accomplished by rotating the HLA to a new orientation. The problem can be modelled as two nonlinear equations in two unknowns. A closed-form solution is presented for the case of stationary source and receiver. Error bounds on the estimates can be calculated as a function of observation errors, HLA rotation angle, and signal arrival geometry. For small observation errors, the resulting errors in the estimated angles can also be expressed in closed form.

1

2　The HLA Bearing Bias Problem

Figure 2.1 illustrates the geometry of a plane wave signal arriving at a Horizontal Line Array. The HLA is lying in the plane $\phi = 0$. The azimuthal angle θ is measured in the plane, clockwise from the HLA axis. The arriving signal has azimuthal angle θ and vertical arrival angle ϕ.

The HLA sensors may be processed using one of several methods, to provide an estimate of $\cos\beta$, where β is the angle of incidence between the array axis and the signal vector [Walker, 1985]. The angle of incidence is a function of the azimuthal angle and the vertical angle:

$$\cos\beta = \cos\theta\cos\phi. \tag{2.1}$$

The estimate of arrival direction therefore has a left-right ambiguity:

$$\beta = \pm\beta_0 \tag{2.2}$$

where

$$\beta_0 = \cos^{-1}\left(\cos\theta\cos\phi\right) \quad ; \quad 0 \le \beta_0 \le 180° . \tag{2.3}$$

If the signal vector is in the plane $\phi = 0$, then $\cos\beta = \cos\theta$. However, if the vertical arrival angle ϕ is non-zero, then the measured angle of incidence β may not be equal to the azimuthal angle θ. β is therefore a biased estimator of θ. The effect of non-zero ϕ is to make $\cos\beta$ smaller than $\cos\theta$. Therefore β is biased toward the broadside direction $\cos\beta = 0$.

A graph will be used to show the magnitude of the bias, for θ between 0° and 180°. The bias, B, is defined as follows:

$$\begin{aligned}
B = \ & \beta - \theta \\
= \ & \cos^{-1}(\cos\theta\cos\phi) - \theta \quad ; \quad 0° \le \theta \le 180° \\
= \ & -\cos^{-1}(\cos\theta\cos\phi) - \theta \quad ; \quad -180° < \theta < 0° .
\end{aligned} \tag{2.4}$$

Figure 2.2 shows the bias error B as a function of θ, for several values of the vertical arrival angle ϕ. It is evident from this figure that bearing bias can be a serious problem. The maximum bias occurs in the endfire directions, $\theta = 0°$ and $\theta = 180°$; the maximum absolute bias error is equal to the vertical arrival angle $|\phi|$:
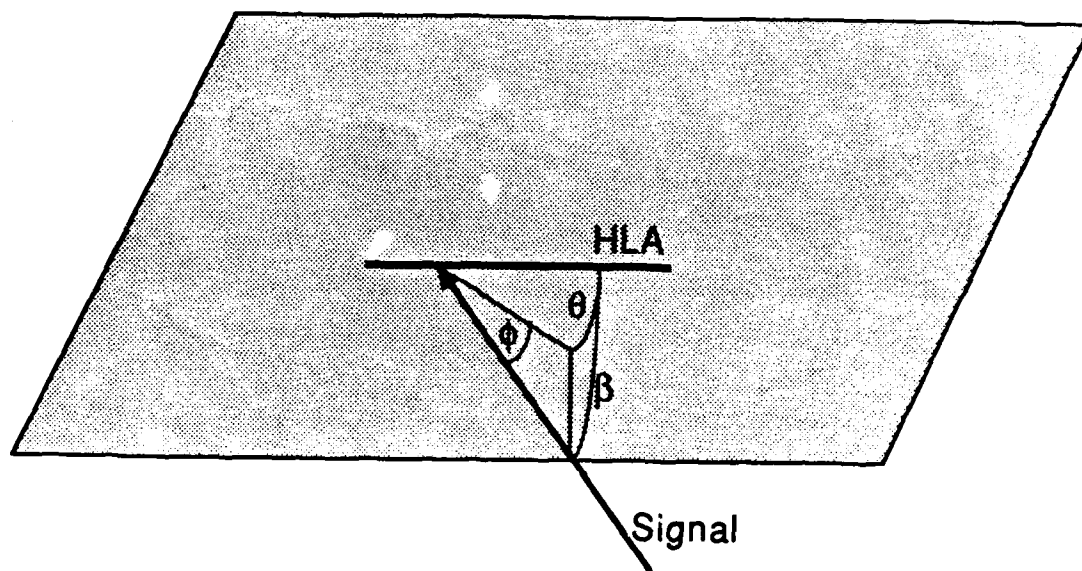
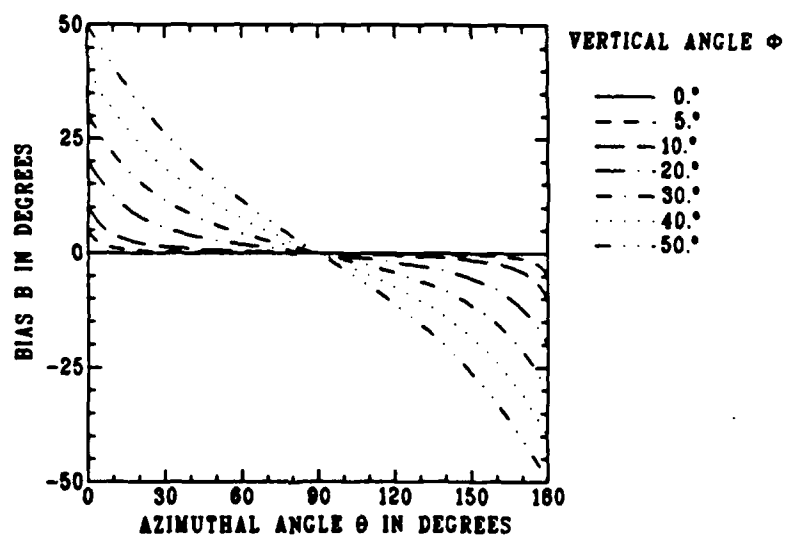$$|B| \le |\phi| . \tag{2.5}$$

2

Figure 2.1: Arrival Angle Geometry

Figure 2.2: HLA Bearing Bias as a function of azimuthal angle θ, for several values of the vertical arrival angle ϕ.

3

3 Estimation of Azimuthal and Vertical Arrival Angles

3.1 Solution by Rotation of the Array

The true azimuthal angle and the vertical arrival angle may both be estimated if a second observation is made. This can be accomplished by rotating the Horizontal Line Array to a new orientation. The problem may then be approximated as two nonlinear equations in two unknowns. A closed-form solution can be obtained for the case of stationary source and receiver. For small errors in the observations and in the assumed rotation angle, the resulting errors in the estimated angles can also be expressed in closed form.

3.2 Assumptions and Restrictions

A number of simplifying assumptions are made in order to find a computable closed-form solution:

(a) The array is assumed to be perfectly stable; errors due to tilting and stretching of the array are not included. However, the standard deviation of the angular observation error may be increased to approximate this effect.

(b) The source and receiver positions are assumed to be stationary. However, the effect of minor relative motion may be approximated by enlarging the error bounds for the final estimated angles.

(c) The propagation path is assumed to be the same for both observations; that is, the vertical arrival angle ϕ remains constant. This assumption restricts the usefulness of the method to environments in which the vertical arrival angle is stable.

(d) The rotation angle $\Delta\theta$ is assumed to be larger than the magnitude of the observation errors ϵ, i.e. $|\sin\Delta\theta| \gg \epsilon$.

4

3.3 The Analytic Model

The Horizontal Line Array is rotated through an angle $\Delta\theta$, where $\sin\Delta\theta \neq 0$. The observations $\cos\beta_1$ and $\cos\beta_2$ are made before and after rotation, respectively. Let θ_1 and θ_2 be the azimuthal angles clockwise from the array forward endfire direction before and after rotation. Let ϕ_1 and ϕ_2 be the corresponding vertical arrival angles before and after rotation. Then it is possible to describe the problem by two equations in four unknowns:

$$\cos\beta_1 = \cos\theta_1\cos\phi_1 \tag{3.1}$$

$$\cos\beta_2 = \cos\theta_2\cos\phi_2 . \tag{3.2}$$

The number of unknowns may be reduced by assuming $\phi_1 = \phi_2 = \phi$ and $\theta_1 = \theta$, $\theta_2 = \theta - \Delta\theta$, to obtain two equations in two unknowns:

$$\cos\beta_1 = \cos\theta\cos\phi \tag{3.3}$$

$$\cos\beta_2 = \cos(\theta - \Delta\theta)\cos\phi. \tag{3.4}$$

The assumption of constant vertical arrival angle ϕ is reasonable if the measurements are made simultaneously by a pair of collocated HLAs, or if the acoustic propagation path is stable. For instance, in underwater acoustics, bottom reflected paths arriving at steep vertical angles are relatively stable.

The assumption of constant azimuthal angle θ is reasonable if there is little relative movement of source and receiver between observations. That is,

(a) the measurements are made simultaneously by a pair of collocated HLAs, or

(b) the source and receiver are stationary, or

(c) the source is in the far field.

In practice, a finite amount of time Δt would be required to rotate the array. The array may also be shifted a distance D. Therefore an error E_θ may be introduced in the estimate of θ due to motion of a source with velocity V at range R:

$$E_\theta \overset{<}{\approx} \frac{180}{\pi}\left(\frac{D + V\Delta t}{R}\right). \tag{3.5}$$

This error should be included when calculating the total error in the final estimate of θ. For example, if $D = 0.075nm$, $V = 1kt$, $\Delta t = 0.1hr$ and $R = 3nm$, then $E_\theta \approx 3.3°$.

5

3.4   The Analytic Solution

The analytic solution may be found by expanding equation 3.4 to obtain:

$$\cos\theta\cos\phi = \cos\beta_1 \tag{3.6}$$

$$\sin\theta\cos\phi = \frac{\cos\beta_2 - \cos\beta_1\cos\Delta\theta}{\sin\Delta\theta} \quad . \tag{3.7}$$

The vertical arrival angle ϕ is found by squaring and summing equations 3.6 and 3.7 to obtain:

$$\cos\phi = \left[(\cos\beta_1)^2 + \left(\frac{\cos\beta_2 - \cos\beta_1\cos\Delta\theta}{\sin\Delta\theta}\right)^2\right]^{\frac{1}{2}} \quad ; \quad 0 \le \phi \le 90 \quad . \tag{3.8}$$

If $\cos\phi \ne 0$, then the azimuthal angle θ is uniquely defined by:

$$\begin{aligned}
\cos\theta &= \cos\beta_1/\cos\phi \\
\sin\theta &= (\cos\beta_2 - \cos\beta_1\cos\Delta\theta)/(\sin\Delta\theta\cos\phi) \quad .
\end{aligned} \tag{3.9}$$

If $\phi = 90°$, then θ is indeterminate. Also, when observation errors are present, care must be taken to ensure that $|\cos\phi|$, $|\cos\theta|$ and $|\sin\theta|$ do not exceed unity.

The next section shows graphs of the relationship between β_1, β_2 and ϕ, and illustrates the sensitivity of the solution to problem geometry.

Section 5 returns to the analytic solution to derive closed-form expressions for maximum and r.m.s. errors in the estimated values of azimuthal angle θ and the cosine of the vertical angle ϕ.

6

4 Graphic Representation

4.1 Graphic Estimation of Vertical Arrival Angle

The HLA angle estimation problem can be solved directly using a computer. However, it is instructive to examine graphs of the relationships between the parameters of interest. Such graphs provide an appreciation for the sensitivity of the solution to observation errors. Graphs may also provide an alternative to using a computer. However, the use of such graphs may be cumbersome due to the large number of variables (β_1, β_2, $\Delta\theta$, θ, and ϕ).

To obtain a graphic solution, it is convenient to first estimate the vertical angle ϕ. There are several ways to solve graphically for ϕ. Four methods will be considered here. In each of these methods, separate graphs are required corresponding to discrete values of the rotation angle $\Delta\theta$.

Method (a) In this method, β_1 is plotted against β_2 for several discrete values of ϕ. This allows graphic resolution of left-right ambiguity, but requires a quadrant search for the correct solution.

Method (b) This method uses absolute angles only. $|\beta_1|$ is plotted against $|\beta_2|$ for several discrete values of ϕ. This graph may also be used to resolve left-right amibiguity, but requires careful interpretation. The larger scale is easier to read.

Method (c) This method uses a nonlinear scale. $\cos\beta_1$ is plotted against $\cos\beta_2$ for several discrete values of ϕ. This is similar to Method (b), except for the use of the cosine scale. Horizontal Line Array resolution capability is usually uniform in the cosine domain. That is, $\cos\beta$ can be estimated with an accuracy which is independent of β. The graph for Method (c) therefore provides a better feeling for sensitivity to observation errors.

Method (d) This method is based on the deviation between the expected and observed values of $|\beta_2|$. Given the observation $|\beta_1|$, two forecasts are made for $|\beta_2|$, for right and left bearing hypotheses, under the assumption that $\phi = 0$. After rotation, the forecast which agrees most closely with the observed value $|\beta_2|$ determines the choice of right or left bearing. If the agreement is not exact, the difference may be used to estimate the magnitude of ϕ. This method allows large values of ϕ to be identified.

7

4.1.1 Example of Method (a)

Figure 4.1 shows the graphs for Method (a), for rotation angles of $20°, 45°$, and $90°$. The observed values of $\cos \beta_1$ and $\cos \beta_2$ do not immediately indicate the signs of these angles. However, for any pair of observations, there is only one signed pair that fits the data. The answer is found by searching through the four possible sign pairs:

$$(+|\beta_1|, \quad +|\beta_2|)$$
$$(+|\beta_1|, \quad -|\beta_2|)$$
$$(-|\beta_1|, \quad +|\beta_2|)$$
$$(-|\beta_1|, \quad -|\beta_2|)$$

Consider the following example:

$$\Delta\theta = 20°, \quad |\beta_1| = 96.4°, \quad |\beta_2| = 108.8°$$

In figure 4.1, the only solution pair is:

$$\beta_1 = -96.4°, \quad \beta_2 = -108.8°$$

which lies on the contour $\phi = 50°$. These values are difficult to read unless the plot is quite large. The estimated azimuthal angles, from Figure 4.5, are:

$$\theta_1 = -100°, \quad \theta_2 = -120°.$$

4.1.2 Example of Method (b)

Figure 4.2 shows the corresponding graphs for Method (b). Given $|\beta_1|$ and $\beta_2|$ as before, the vertical angle ϕ may be read from the graph by interpolating between contours. This graph is easier to read because the contours are continuous and are plotted on a larger scale. The left-right ambiguity is resolved as follows. For any given vertical angle ϕ, there are two possible a priori values of $|\beta_2|$ for each observed angle β_1. The largest value corresponds to rotation away from the signal direction (θ_1 and $\Delta\theta$ have opposite signs); the smallest value corresponds to rotation towards the signal direction (θ_1 and $\Delta\theta$ have the same sign).

4.1.3 Example of Method (c)

Figure 4.3 shows the graphs for Method (c). The vertical angle ϕ and the left-right ambiguity may be solved as for Method (b). The natural cosine scale gives a better appreciation of the ability to resolve different values of ϕ. For instance, a large value of ϕ produces a large shift in the observed value β_1 when the signal is arriving from the endfire directions $\theta = 0°$ and $\theta = 180°$; however the HLA is less capable of resolving these differences in the endfire directions.
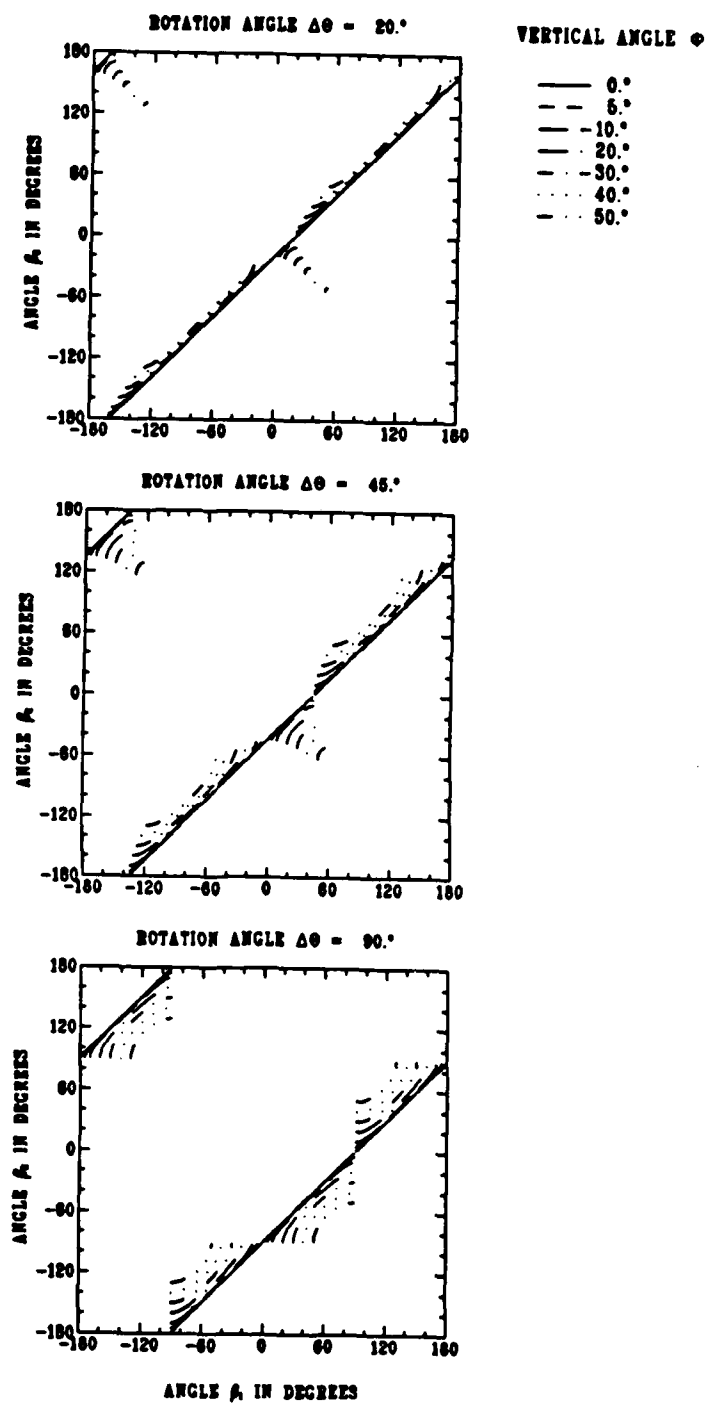
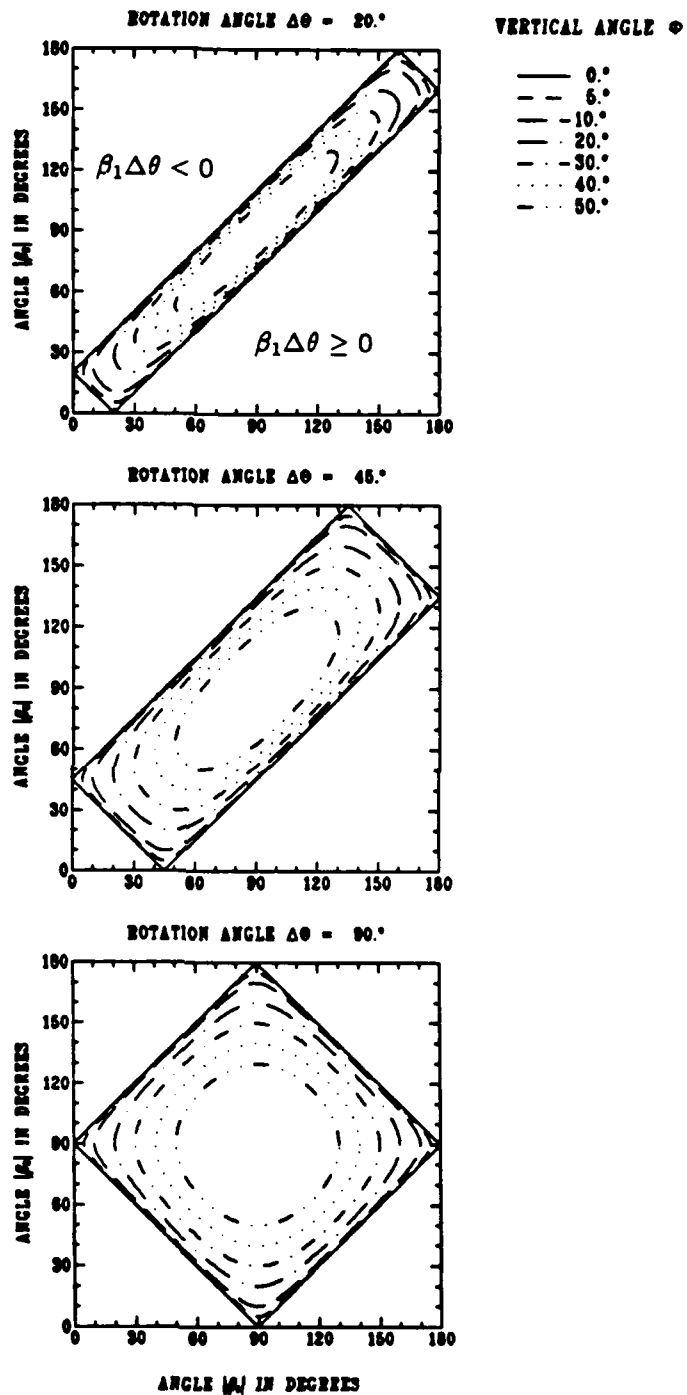Figure 4.1: Estimation of vertical arrival angle ϕ using graphic Method (a)

Figure 4.2: Estimation of vertical arrival angle ϕ using graphic Method (b)

ROTATION ANGLE Δθ = 20.°

VERTICAL ANGLE φ

$\beta_1 \Delta\theta < 0$

$\beta_1 \Delta\theta \geq 0$

ROTATION ANGLE Δθ = 45.°

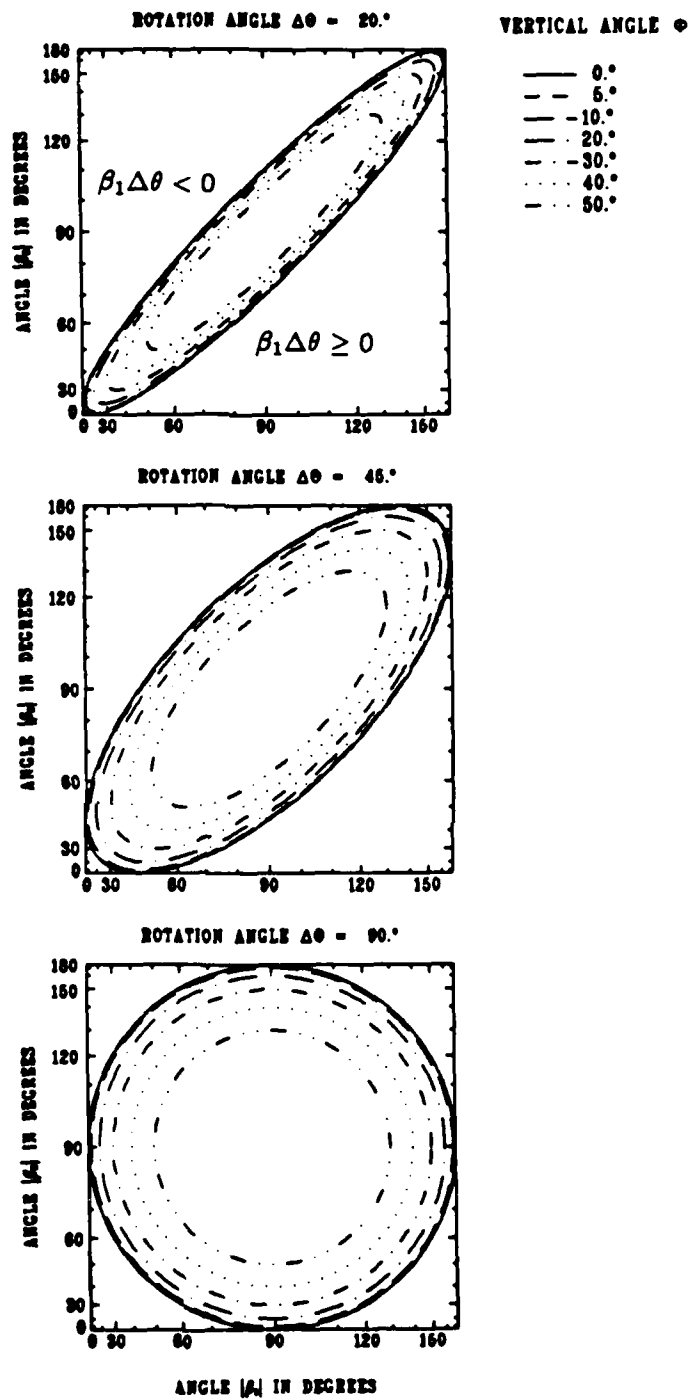ROTATION ANGLE Δθ = 90.°

ANGLE |φ| IN DEGREES

Figure 4.3: Estimation of vertical arrival angle ϕ using graphic Method (c)

11

4.1.4 Example of Method (d)

Figure 4.4 shows the graphs for Method (d). In this Method, the a priori estimate $|\hat{\beta}_2|$, is based on the assumption that the vertical arrival angle ϕ is equal to 0. There are two possible solutions, corresponding to the ambiguous left and right solutions:

$$|\hat{\beta}_2|^{(a)} = \cos^{-1}\left(\cos(|\beta_1| + |\Delta\theta|)\right) \quad ; \quad \Rightarrow \beta_1\Delta\theta < 0 \tag{4.1}$$

or

$$|\hat{\beta}_2|^{(b)} = \cos^{-1}\left(\cos(|\beta_1| - |\Delta\theta|)\right) \quad ; \quad \Rightarrow \beta_1\Delta\theta \geq 0 \ . \tag{4.2}$$

After the observation $|\beta_2|$, the chosen estimate $|\hat{\beta}_2|$ is the one which agrees most closely with the observation. The deviation δ is then defined as follows:

$$\delta = |\beta_2| - |\hat{\beta}_2| \tag{4.3}$$

Note, in Figure 4.2, that zero deviation is expected when $\phi = 0$. If $\phi \neq 0$, then a negative deviation is expected when the rotation is away from the signal direction; a positive deviation is expected when the rotation is towards the signal direction.

Consider the same example again:

$$\Delta\theta = 20°, \ |\beta_1| = 96.4° \text{ and } |\beta_2| = 108.8°$$

Then:

$$|\hat{\beta}_2|^{(a)} = 116.4° \text{ and } |\hat{\beta}_2|^{(b)} = 76.4°$$

The appropriate choice is

$$|\hat{\beta}_2| = |\hat{\beta}_2|^{(a)} = 116.4°,$$

which implies that $\beta_1\Delta\theta < 0$ and therefore

$$\beta_1 = -96.4°.$$

However, there is not a perfect match between the predicted angle before rotation and the observed angle after rotation. The deviation is:

$$\delta = |108.8°| - |116.4°| = -7.6°.$$

From Figure 4.4, the value of the vertical arrival angle ϕ is therefore 50°. Note that in Figure 4.4, the derivative discontinuties correspond to the corners of the rectangles in Figure 4.2.
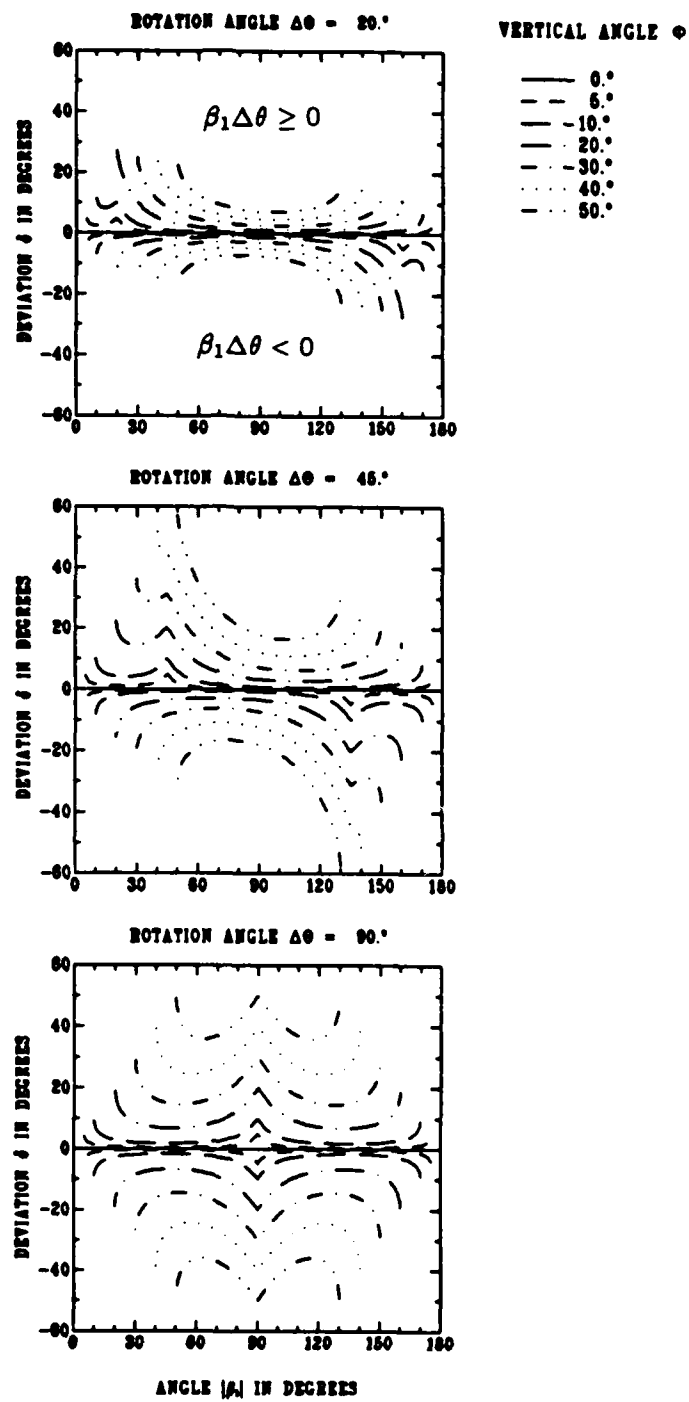
12

Figure 4.4: Estimation of vertical arrival angle ϕ using graphic Method (d)

13

4.2 Graphic Estimation of Azimuthal Angle

Once the value of the vertical arrival angle ϕ has been estimated, it may then be used to correct β to estimate the true bearing θ. Equation 2.1 defines the relationship between θ, ϕ and β. Figure 4.5 shows the relationship between θ and β for several values of ϕ.

To continue the example from the preceding section, it has been shown that, if

$$\Delta\theta = 20°, \ |\beta_1| = 96.4°, \ \text{and} \ |\beta_2| = 108.8°,$$

then it can be deduced that

$$\beta_1 = -96.4°, \ \beta_2 = -108.8°, \ \text{and} \ \phi = 50° \ .$$

Equation 2.1 or Figure 4.5 may be used to obtain the estimated azimuthal angles:

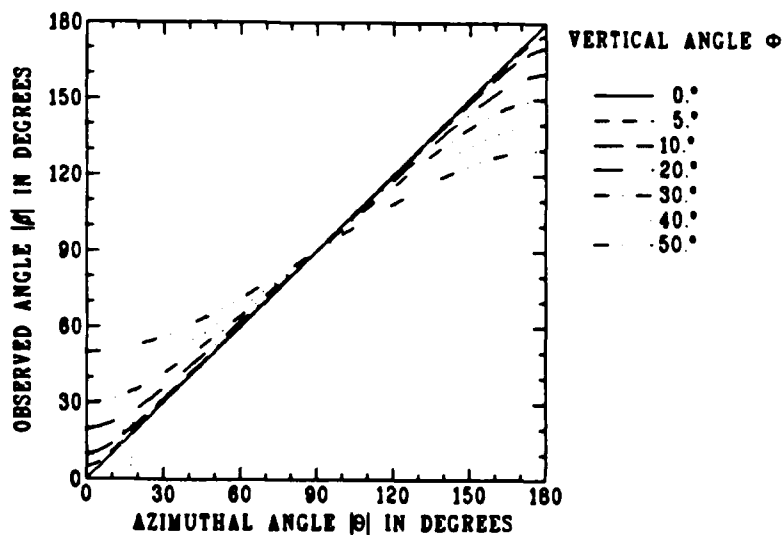$$\theta_1 = -100°, \ \theta_2 = -120° \ .$$

Figure 4.5: The true bearing θ can be obtained from observation β, if the vertical angle ϕ is known.

14

5 Error Estimates

5.1 Model of Observation Errors

The analytic solution provides an exact closed form for the azimuthal and vertical arrival angles. However there may be errors in the observed values $\cos\beta_1$ and $\cos\beta_2$ as well as error in the assumed rotation angle $\Delta\theta$.

5.1.1 Errors in $\cos\beta$

It will be assumed that the standard deviation of the HLA observation $\cos\beta$ is independent of β:

$$\sigma_{\cos\beta} = \epsilon = \sin\sigma_0 \tag{5.1}$$

where σ_0 is the standard deviation of the bearing error in the broadside direction $|\beta| = 90°$, for a specified signal-to-noise ratio. Figure 5.1 shows the observation errors $\Delta\beta$ corresponding to $\cos\beta \pm \epsilon$ as a function of β for the case $\sigma_0 = 1°$. Note that maximum errors $|\Delta\beta|_{max}$ occur in the endfire directions, and also at angles $0 + |\Delta\beta|_{max}$ and $180 - |\Delta\beta|_{max}$. For small values of ϵ, a second-order Taylor series expansion of $\cos\beta$ leads to an approximate expression for $|\Delta\beta|_{max}$:

$$\Delta\cos\beta \approx -\sin\beta\left(\frac{\pi}{180}\Delta\beta\right) - \frac{1}{2}\cos\beta\left(\frac{\pi}{180}\Delta\beta\right)^2 \tag{5.2}$$

$$\frac{\pi}{180}\Delta\beta \approx \frac{-\sin\beta + \text{sign}(\sin\beta)\sqrt{(\sin^2\beta \pm 2\cos\beta\Delta\cos\beta)^+}}{\cos\beta} \quad ; \quad \cos\beta \neq 0 \tag{5.3}$$

$$\frac{\pi}{180}|\Delta\beta|_{max} \approx \sqrt{2\epsilon} \tag{5.4}$$

$$|\Delta\beta|_{max} \approx \sqrt{\frac{180}{\pi}2\sigma_0} \approx 10.7\sqrt{\sigma_0} \quad . \tag{5.5}$$
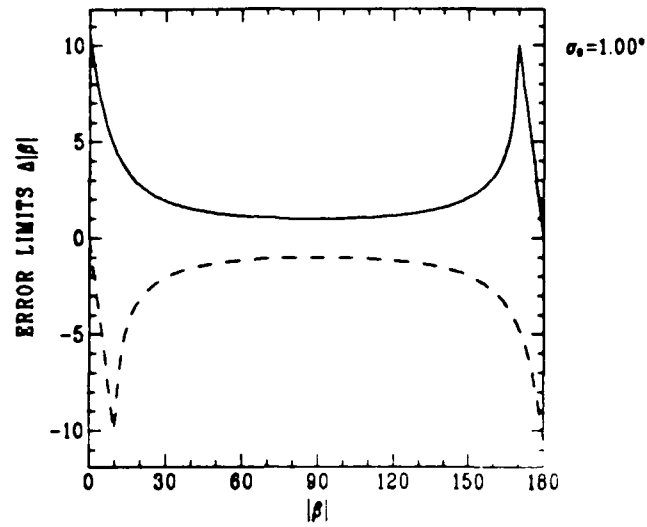
In this example, the maximum error is approximately 10.7°.

15

Figure 5.1: Bounds on error in the observed angle $|\beta|$, corresponding to $\cos\beta \pm \sin\sigma_0$, where $\sigma_0 = 1°$.

5.1.2 Errors in Rotation Angle $\Delta\theta$

The standard deviation in the rotation angle $\Delta\theta$ will be denoted by

$$\sigma_{\Delta\theta} = h \qquad (5.6)$$

where h is given in degrees.

16

5.2 Resulting Errors in the Closed-Form Solution

For suitably small errors ϵ and h, the resulting errors in the estimated azimuthal and vertical arrival angles θ and ϕ can be approximated in closed form. However, if the errors are large, more elaborate methods are required to estimate the errors [Theriault, 1987].

First derivatives are obtained by differentiating equations 3.6 and 3.8 with respect to $\cos \beta_1$, $\cos \beta_2$ and $\Delta \theta$ to obtain the following expressions:

$$\frac{\partial \cos \phi}{\partial \cos \beta_1} = -\frac{\sin \theta_2}{\sin \Delta \theta} \qquad (5.7)$$

$$\frac{\partial \cos \phi}{\partial \cos \beta_2} = \frac{\sin \theta_1}{\sin \Delta \theta} \qquad (5.8)$$

$$\frac{\partial \cos \phi}{\partial \Delta \theta} = -\frac{\pi}{180} \frac{\sin \theta_1 \sin \theta_2 \cos \phi}{\sin \Delta \theta} \qquad (5.9)$$

$$\frac{\partial \theta_1}{\partial \cos \beta_1} = -\frac{180}{\pi} \frac{\cos \theta_2}{\cos \phi \sin \Delta \theta} \qquad (5.10)$$

$$\frac{\partial \theta_1}{\partial \cos \beta_2} = \frac{180}{\pi} \frac{\cos \theta_1}{\cos \phi \sin \Delta \theta} \qquad (5.11)$$

$$\frac{\partial \theta_1}{\partial \Delta \theta} = -\frac{\cos \theta_1 \sin \theta_2}{\sin \Delta \theta} \qquad (5.12)$$

The error analysis is based on a first-order Taylor series expansion in the errors ϵ and h. It is assumed that these errors are small with respect to the rotation angle:

$$\begin{aligned} \epsilon = \sin \sigma_0 &\ll |\sin \Delta \theta| \cos \phi \\ \frac{\pi}{180} h &\ll |\sin \Delta \theta| \ . \end{aligned} \qquad (5.13)$$

It is further assumed that the errors in $\cos \beta_1$, $\cos \beta_2$, and the error in the assumed rotation angle $\Delta \theta$, are statistically independent. Two cases will be considered here:— maximum errors and root-mean-square errors.

5.2.1 Maximum Errors

It will be assumed that ϵ and h are strict upper bounds on the errors in $\cos \beta$ and $\Delta \theta$:

$$\begin{aligned} |\hat{\cos} \beta - \cos \beta| &\leq \epsilon \\ |\hat{\Delta \theta} - \Delta \theta| &\leq h \ . \end{aligned} \qquad (5.14)$$

17

Then upper bounds on the absolute errors in the vertical angle $\cos\phi$ and the azimuthal angle θ are given by the first-order Taylor expansions:

$$|\hat{\cos}\phi - \cos\phi| \overset{<}{\approx} \left|\frac{\partial\cos\phi}{\partial\cos\beta_1}\right|\varepsilon + \left|\frac{\partial\cos\phi}{\partial\cos\beta_2}\right|\varepsilon + \left|\frac{\partial\cos\phi}{\partial\Delta\theta}\right|h$$

$$\overset{<}{\approx} \left[\frac{|\sin\theta_1| + |\sin\theta_2|}{|\sin\Delta\theta|}\right]\varepsilon + \frac{\pi}{180}\left|\frac{\sin\theta_1\sin\theta_2\cos\phi}{\sin\Delta\theta}\right|h \tag{5.15}$$

$$= U_{\cos\phi}$$

$$\frac{\pi}{180}|\hat{\theta} - \theta| \overset{<}{\approx} \left|\frac{\partial\theta_1}{\partial\cos\beta_1}\right|\varepsilon + \left|\frac{\partial\theta_1}{\partial\cos\beta_2}\right|\varepsilon + \left|\frac{\partial\theta_1}{\partial\Delta\theta}\right|h$$

$$\overset{<}{\approx} \left[\frac{|\cos\theta_1| + |\cos\theta_2|}{|\sin\Delta\theta|\cos\phi}\right]\varepsilon + \frac{\pi}{180}\left|\frac{\cos\theta_1\sin\theta_2}{\sin\Delta\theta}\right|h \tag{5.16}$$

$$= U_\theta \ .$$

Annex A contains a parametric analysis of maximum errors.

5.2.2 R.M.S. Errors

The r.m.s. errors of the estimated azimuthal angle and the cosine of the vertical angle will be denoted by S_θ and $S_{\cos\phi}$ respectively. For small error standard deviations ε and h, a first-order Taylor series expansion may be used to obtain the following estimated errors:

$$S_{\cos\phi} \approx \left[\left(\frac{\partial\cos\phi}{\partial\cos\beta_1}\varepsilon\right)^2 + \left(\frac{\partial\cos\phi}{\partial\cos\beta_2}\varepsilon\right)^2 + \left(\frac{\partial\cos\phi}{\partial\Delta\theta}h\right)^2\right]^{1/2}$$

$$\approx \frac{\left[(\sin^2\theta_1 + \sin^2\theta_2)\varepsilon^2 + (\frac{\pi}{180}\sin\theta_1\sin\theta_2\cos\phi)^2h^2\right]^{1/2}}{|\sin\Delta\theta|} \tag{5.17}$$

$$\frac{\pi}{180}S_\theta \approx \left[\left(\frac{\partial\theta_1}{\partial\cos\beta_1}\varepsilon\right)^2 + \left(\frac{\partial\theta_1}{\partial\cos\beta_2}\varepsilon\right)^2 + \left(\frac{\partial\theta_1}{\partial\Delta\theta}h\right)^2\right]^{1/2}$$

$$\approx \frac{\left[(\cos^2\theta_1 + \cos^2\theta_2)\varepsilon^2 + (\frac{\pi}{180}\cos\theta_1\sin\theta_2\cos\phi)^2h^2\right]^{1/2}}{|\sin\Delta\theta|\cos\phi} \tag{5.18}$$

Note that the approximate error in $\cos\phi$ is not exact as ϕ approaches zero because of the boundary constraint $|\cos\phi| \leq 1$. Similarly, the approximate error in θ is not exact as

β approaches the endfire directions. In these situations, the approximate error expression overestimates the actual r.m.s. error.

From these equations, the effect of an error h in the rotation angle is comparable to the effect of the broadside angular resolution σ_0. Therefore, if $h\cos\phi > \sigma_0$ then the error in rotation angle dominates, while if $h\cos\phi < \sigma_0$ the angular resolution of the array dominates. Errors in the rotation angle are less critical when the vertical arrival angle is steep.

Annex B contains a parametric analysis of r.m.s. errors. Annex C contains examples of the effect of error in rotation angle.

5.3 An Example of Maximum Errors

5.3.1 Errors When Vertical Angle Bias is Not Removed

First, for purposes of comparison, it is instructive to consider the errors which occur if the array is not rotated, and the vertical arrival angle ϕ is assumed to be zero. For the special case $\Delta\theta = 0$, the maximum errors are defined as follows:

$$U_\theta \approx |B(\theta,\phi)| + |\Delta\beta(\theta,\phi,\epsilon)| + h \quad ; \quad \Delta\theta = 0 \tag{5.19}$$

$$U_\phi = \phi \quad ; \quad \Delta\theta = 0 \tag{5.20}$$

Figure 5.2 shows the approximate error bound U_θ on azimuthal angle, for $\phi = 20°$. The broadside resolution angle is $\sigma_0 = 1°$, and the error h in rotation angle is assumed to be zero. The error is most severe in the endfire directions. At endfire, the estimates are subject to the maximum bias error plus the maximum angular resolution and rotation angle error.

5.3.2 Errors in Estimated Azimuthal Angle after Rotation

Figure 5.3 shows a plot of the resulting error bound U_θ in the azimuthal angle estimate as a function of the true azimuthal angle θ, for rotation angle $\Delta\theta = 20°$, when the vertical arrival angle is $\phi = 20°$. Note that the maximum error in θ occurs near the endfire directions $\theta = 0°$ and $\theta = 180°$. The minimum errors occur near the broadside directions $\theta = \pm90°$.

5.3.3 Errors in Estimated Vertical Angle after Rotation

Figure 5.4 shows the error in the estimated vertical arrival angle ϕ corresponding to $\cos\phi \pm U_{\cos\phi}$ for the same example. Note that the errors in ϕ have the opposite trend to errors in θ. The minimum error in vertical arrival angle occurs near the endfire directions $\theta = 0°$ and $\theta = 180°$. The maximum errors occur near the broadside directions $\theta = \pm90°$.

ROTATION ANGLE Δθ = 0.°
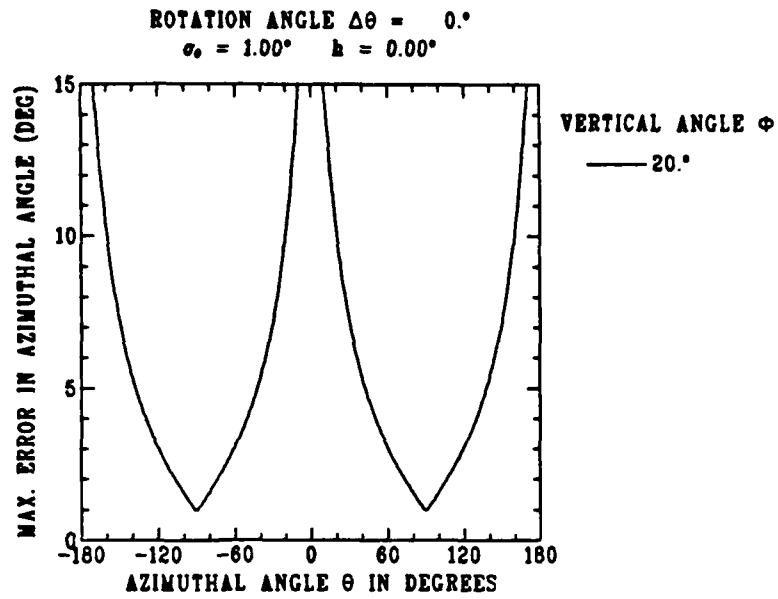σ_ϕ = 1.00°   h = 0.00°

VERTICAL ANGLE Φ

———— 20.°

Figure 5.2: Approximate bound U_θ on error in the estimated azimuthal angle θ when the array is not rotated, and the vertical arrival angle ϕ is assumed to be zero; maximum broadside angular error is $\sigma_0 = 1°$; the error h in rotation angle is zero; the true value of ϕ is 20°.
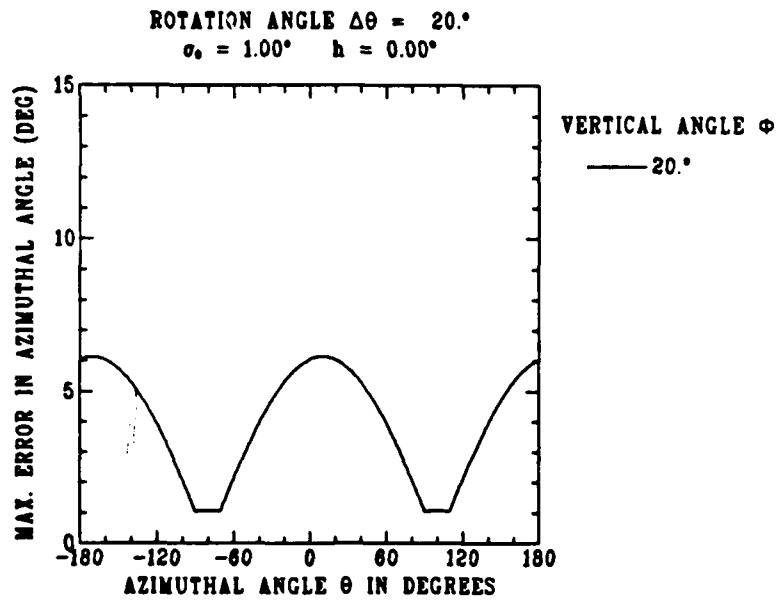

ROTATION ANGLE Δθ = 20.°
σ_ϕ = 1.00°   h = 0.00°

VERTICAL ANGLE Φ

———— 20.°

Figure 5.3: Error bound U_θ for the estimated azimuthal angle θ as a function of θ, for vertical arrival angle $\phi = 20°$; maximum broadside angular error is $\sigma_0 = 1°$; rotation angle $\Delta\theta = 20°$.

20

ROTATION ANGLE $\Delta\theta$ = 20.°
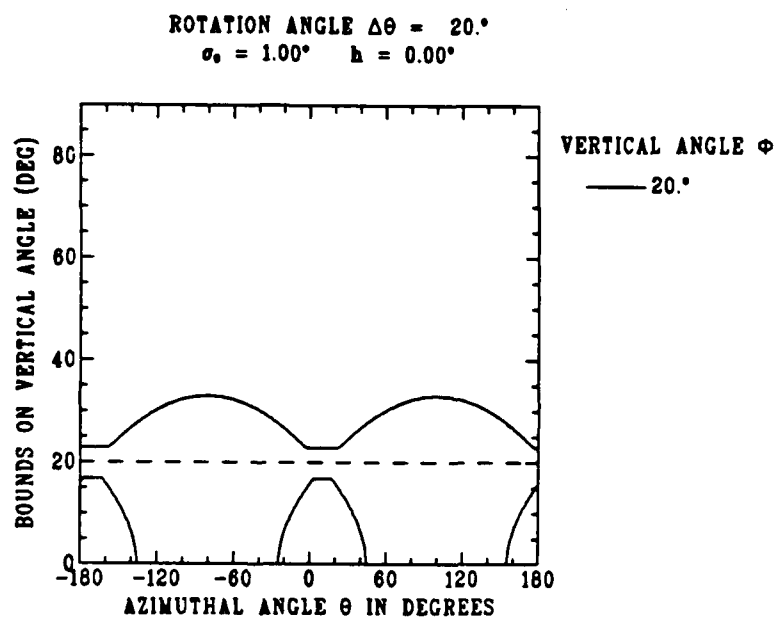$\sigma_\bullet$ = 1.00°   h = 0.00°

VERTICAL ANGLE Φ

——— 20.°

Figure 5.4: Bounds on the estimated vertical arrival angle $\phi = 20°$, as a function of azimuthal angle θ; maximum broadside angular error is $\sigma_0 = 1°$; rotation angle $\Delta\theta = 20°$.

21

5.4 General Trends

Appendix A contains a parametric analysis of error bounds on θ and ϕ resulting from errors in the observations $\cos \beta$. The parametric analysis includes several values of rotation angle $\Delta \theta$ and vertical arrival angle ϕ.

The best azimuthal estimates are obtained near the broadside direction; steep vertical arrival angles degrade the estimate of azimuthal angle. If the initial observed angle is near broadside and the vertical arrival angle is very small, a solution by rotation of the array leads to slightly larger errors than the simple uncorrected estimate. However, since the vertical arrival angle is usually unknown, rotation is recommended. Rotation produces a significant decrease in the estimated azimuthal error, when the vertical angle is steep.

The best vertical angle estimates are obtained near the endfire directions; steep vertical arrival angles improve the estimate of vertical arrival angle.

Appendix B contains a parametric analysis of r.m.s. errors for the same cases. The same general trends apply.

Appendix C contains a parametric analysis of the effect of errors in the rotation angle. Errors in rotation angle produce maximum errors in azimuthal estimates near endfire; these errors are independent of vertical arrival angle. Maximum errors in vertical angle occur near broadside; these errors decrease as the vertical arrival angle increases.

The overall errors are minimized when the rotation angle is $\pm 90°$. In order to make effective use of the rotation solution, the rotation angle must be large with respect to the broadside resolution angle σ_0 and the rotation angle error h.

6 Conclusions

A Horizontal Line Array (HLA) is subject to left-right bearing ambiguity due to its one-dimensional nature. It is also subject to bearing bias error if the signal vector is not in the same plane as the HLA. However, by rotating the array to a new orientation, it is possible to estimate both the azimuthal angle and the vertical arrival angle. The solution is given in closed form, for the case of stationary source and receiver. The method relies on the existence of a stable vertical arrival angle.

Graphic methods may be used to aid in solution. However, a separate graph is required for each possible rotation angle. Graphic methods are also limited in accuracy, since manual interpolation is required. However, graphs provide an appreciation of the sensitivity of the solution to observation errors.

Solution errors can be expressed in closed form as a function of small errors in observed angles and small errors in the angle of rotation. Best estimates of vertical arrival angle are obtained in the endfire directions, with steep vertical arrival angles. Best estimates of azimuthal angle are obtained in the broadside directions, with zero vertical arrival angle. Overall estimates improve as the array rotation angle approaches 90°.

Array rotation can produce significant overall improvement of the azimuthal angle estimate. The effect of large vertical arrival angles is reduced dramatically. However, if the vertical arrival angle is very small, angle estimates near broadside are slightly degraded.

Bibliography

[Walker, 1985]   R. S. Walker, *Bearing Accuracy and Resolution Bounds of High-Resolution Beamformers;* ICASSP-IEEE International Conference on Acoustics, Speech, and Signal Processing; March 26-29, 1985.

[Theriault, 1987] James A. Theriault, *Error Estimates for Azimuthal and Vertical Arrival Angles at a Rotatable Horizontal Line Array;* DREA Technical Memorandum 87/(Draft).

Appendix A Parametric Analysis of Maximum Errors

A number of graphs have been prepared to examine the sensitivity of the analytic solution to worst-case errors in the observed angles. The maximum positive and negative errors in the vertical angle U_ϕ^+ and U_ϕ^- are defined as follows:

$$
\begin{aligned}
U_\phi^+ &= \cos^{-1}(C^+) - \phi \\
U_\phi^- &= \cos^{-1}(C^-) - \phi
\end{aligned}
\tag{A.1}
$$

where

$$
\begin{aligned}
C^+ &= \max\left[(\cos\phi - U_{\cos\phi}),\ 0\right] \\
C^- &= \min\left[(\cos\phi + U_{\cos\phi}),\ 1\right] \quad .
\end{aligned}
\tag{A.2}
$$

It is assumed in all of these cases that the rotation angle is known exactly (i.e. $h = 0$). The maximum angle error at broadside is $\sigma_0 = 1°$. Four rotation angles $20°$, $45°$, $90°$ and $135°$ are considered. Several vertical arrival angles are examined. Section 5.4 discusses the general trends shown in these graphs.

For purposes of comparison, figure A.1 shows the maximum error U_θ for the case where the array is not rotated, and the vertical arrival angle is assumed to be zero.

Figure A.1: Bound U_θ on the maximum error in the estimated azimuthal angle if the array is not rotated; $\sigma_0 = 1°$; $h = 0$.
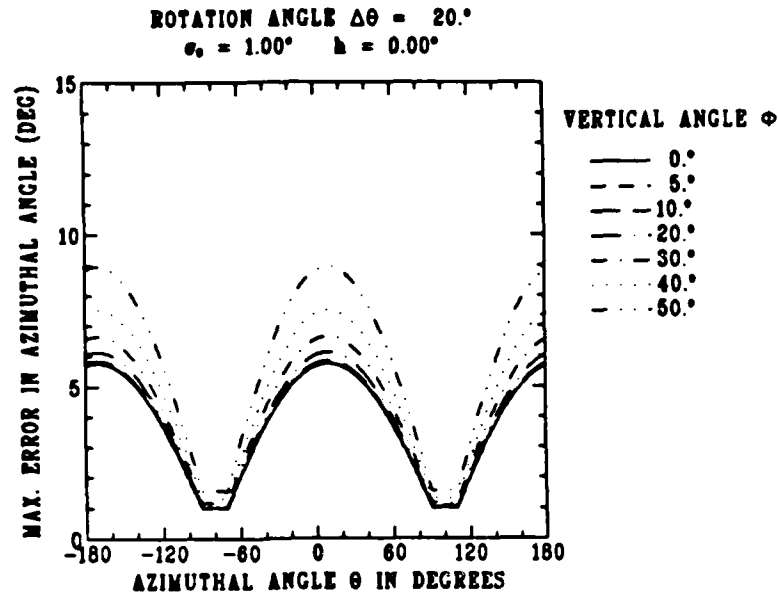
ROTATION ANGLE Δθ = 20.°
σ₀ = 1.00°   h = 0.00°
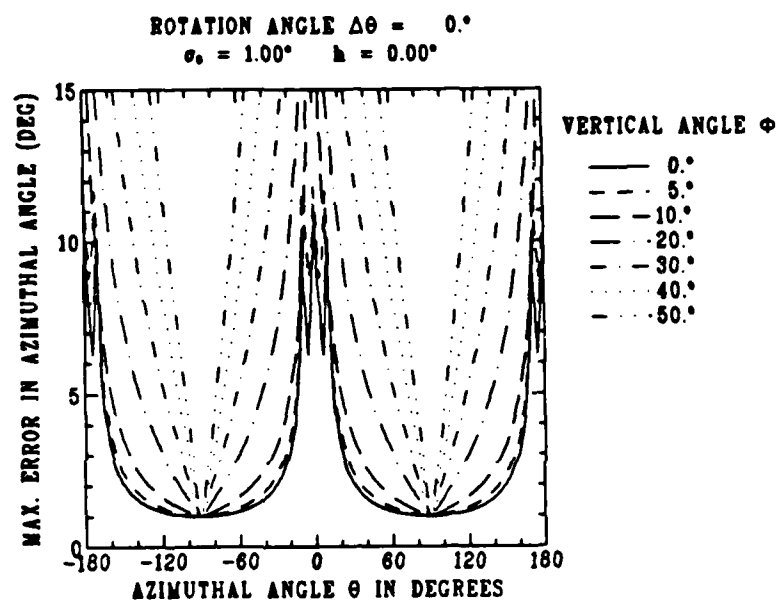
Figure A.2: Error bound U_θ on the estimated azimuthal angle θ, as a function of θ and the vertical arrival angle ϕ, where the maximum cosine error is $\sin \sigma_0$; $\sigma_0 = 1°$; rotation angle $\Delta\theta = 20°$; $h = 0$.
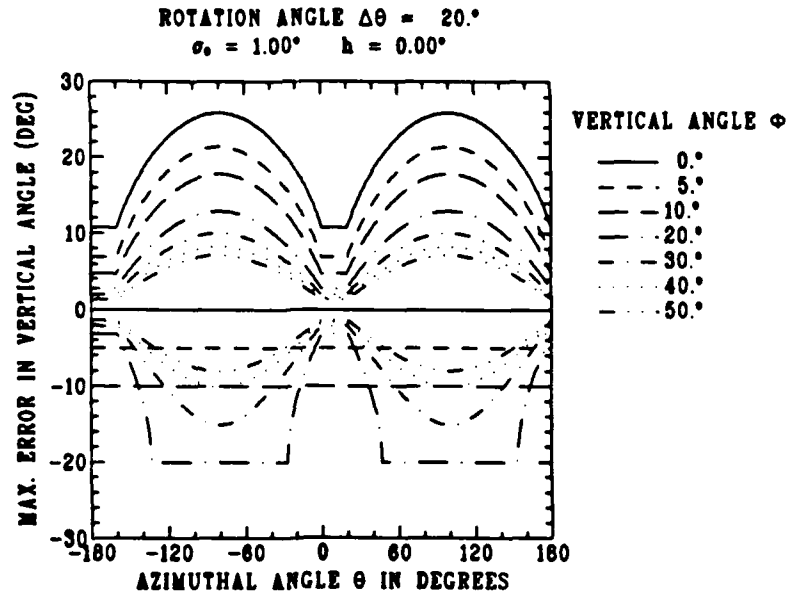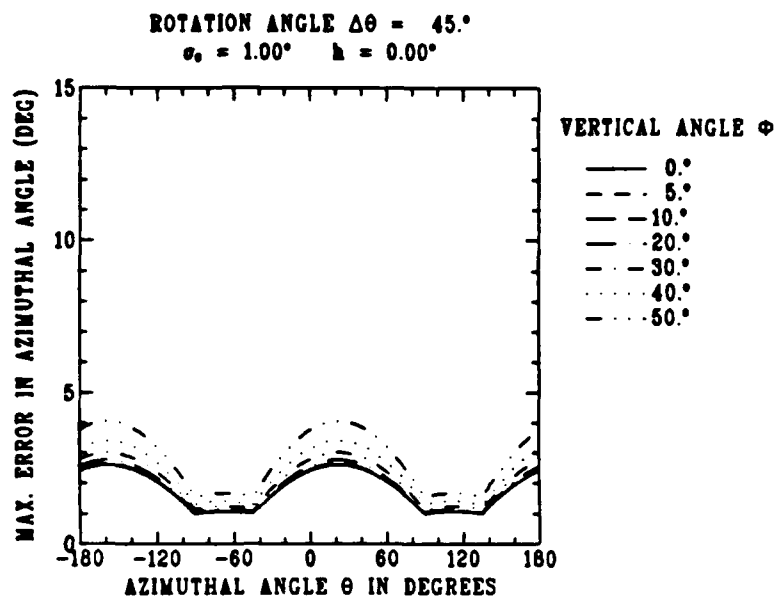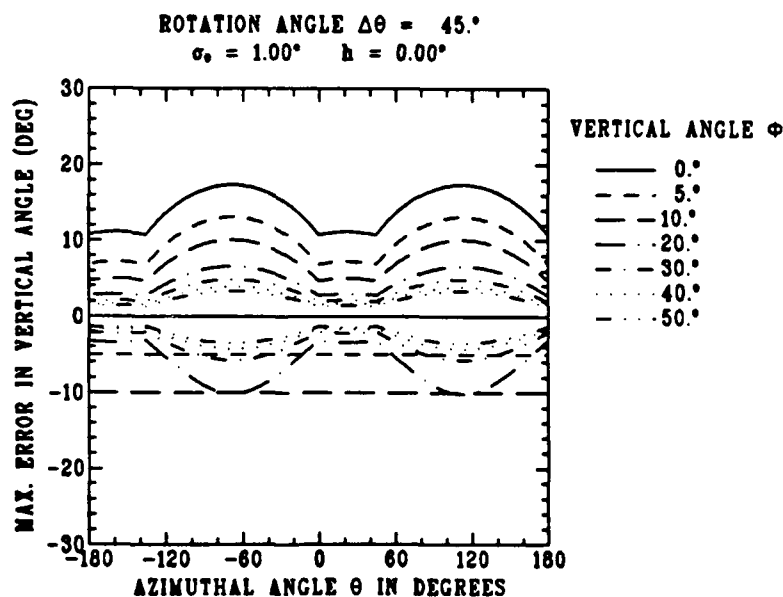
ROTATION ANGLE Δθ = 20.°
σ₀ = 1.00°   h = 0.00°

Figure A.3: Error bounds U_ϕ^+ and U_ϕ^- on the estimated vertical arrival angle ϕ, as a function of azimuthal angle θ, for several vertical arrival angles ϕ, where the maximum cosine error is $\sin \sigma_0$; $\sigma_0 = 1°$; rotation angle $\Delta\theta = 20°$; $h = 0$.
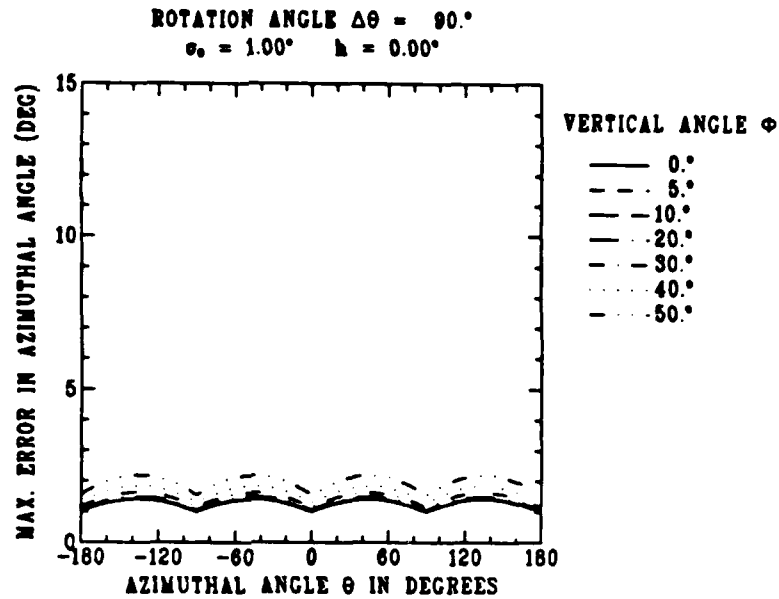
27

ROTATION ANGLE Δθ = 45.°
σ₀ = 1.00°   h = 0.00°

Figure A.4: Error bound U_θ on the estimated azimuthal angle θ, as a function of θ and the vertical arrival angle ϕ, where the maximum cosine error is $\sin\sigma_0$; $\sigma_0 = 1°$; rotation angle $\Delta\theta = 45°$; $h = 0$.
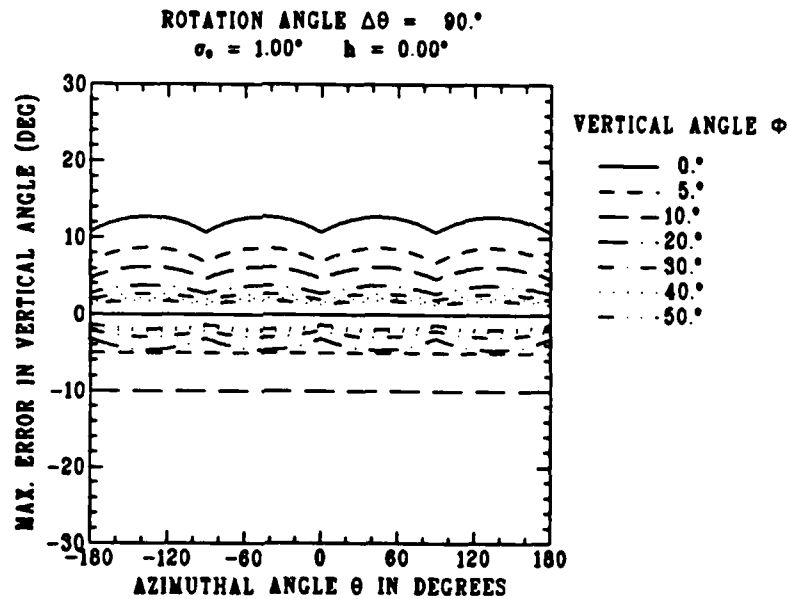

Figure A.5: Error bounds U_ϕ^+ and U_ϕ^- on the estimated vertical arrival angle ϕ, as a function of azimuthal angle θ, for several vertical arrival angles ϕ, where the maximum cosine error is $\sin\sigma_0$; $\sigma_0 = 1°$; rotation angle $\Delta\theta = 45°$; $h = 0$.
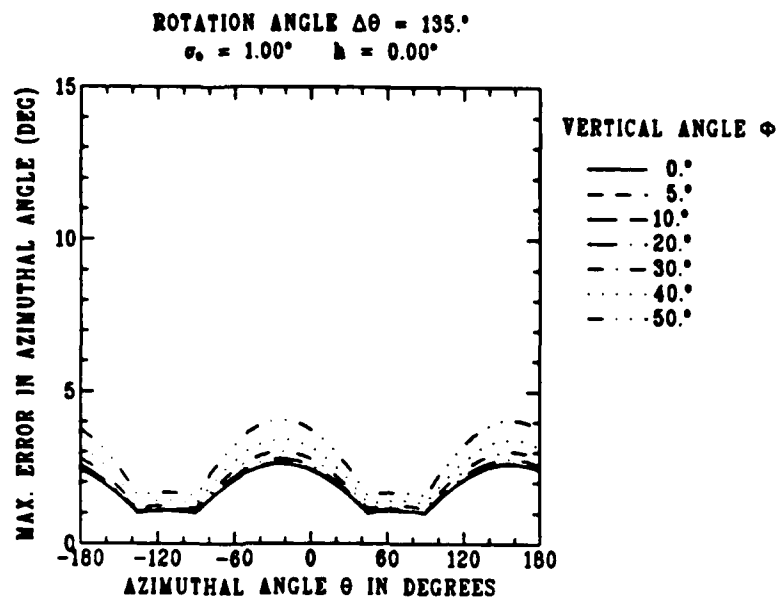
28

ROTATION ANGLE Δθ = 90.°
σ₀ = 1.00°   h = 0.00°

Figure A.6: Error bound U_θ on the estimated azimuthal angle θ, as a function of θ and the vertical arrival angle ϕ, where the maximum cosine error is $\sin \sigma_0$; $\sigma_0 = 1°$; rotation angle $\Delta\theta = 90°$; $h = 0$.
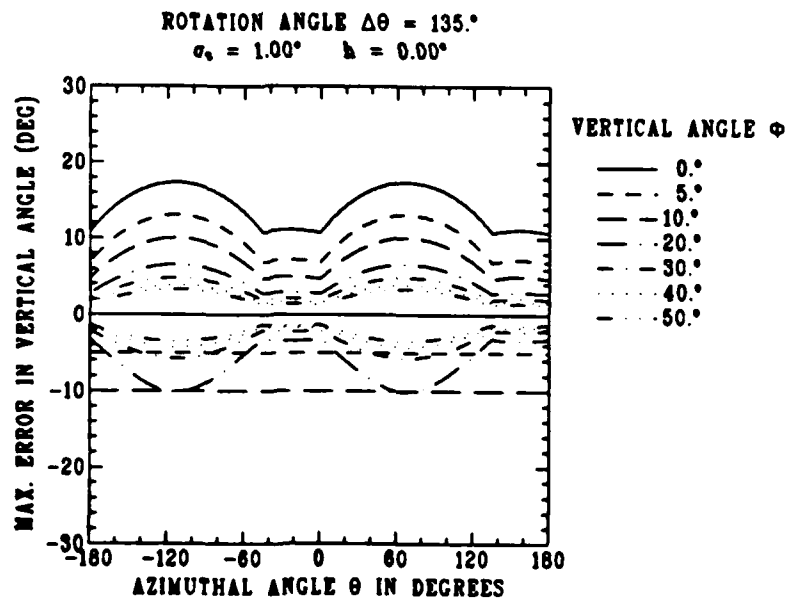

ROTATION ANGLE Δθ = 90.°
σ₀ = 1.00°   h = 0.00°

Figure A.7: Error bounds U_ϕ^+ and U_ϕ^- on the estimated vertical arrival angle ϕ, as a function of azimuthal angle θ, for several vertical arrival angles ϕ, where the maximum cosine error is $\sin \sigma_0$; $\sigma_0 = 1°$; rotation angle $\Delta\theta = 90°$; $h = 0$.

29

ROTATION ANGLE Δθ = 135.°
σ₀ = 1.00°   h = 0.00°

Figure A.8: Error bound U_θ on the estimated azimuthal angle θ, as a function of θ and the vertical arrival angle ϕ, where the maximum cosine error is $\sin\sigma_0$; $\sigma_0 = 1°$; rotation angle $\Delta\theta = 135°$; $h = 0$.

ROTATION ANGLE Δθ = 135.°
σ₀ = 1.00°   h = 0.00°

Figure A.9: Error bounds U_ϕ^+ and U_ϕ^- on the estimated vertical arrival angle ϕ, as a function of azimuthal angle θ, for several vertical arrival angles ϕ, where the maximum cosine error is $\sin\sigma_0$; $\sigma_0 = 1°$; rotation angle $\Delta\theta = 135°$; $h = 0$.

30

Appendix B Parametric Analysis of R.M.S. Errors

A number of graphs have been prepared to examine the sensitivity of the analytic solution to random errors in the observed angles. The positive and negative errors in the vertical angle S_ϕ^+ and S_ϕ^- corresponding to the approximate r.m.s. error $S_{\cos\phi}$ are defined as follows:

$$
\begin{aligned}
S_\phi^+ &= \cos^{-1}(C^+) - \phi \\
S_\phi^- &= \cos^{-1}(C^-) - \phi
\end{aligned}
\tag{B.1}
$$

where

$$
\begin{aligned}
C^+ &= \max\left[(\cos\phi - S_{\cos\phi}),\ 0\right] \\
C^- &= \min\left[(\cos\phi + S_{\cos\phi}),\ 1\right] \ .
\end{aligned}
\tag{B.2}
$$

It is assumed in all of these cases that the rotation angle is known exactly (i.e. $h = 0$). The broadside resolution angle σ_0 is 1°. Four rotation angles 20°, 45°, 90°and 135°are considered. Several vertical arrival angles are examined. Section 5.4 discusses the general trends shown in these graphs.

For purposes of comparison, figure B.1 shows the r.m.s. error S_θ for the case where the array is not rotated, and the vertical arrival angle is assumed to be zero. For this special case, the approximate r.m.s. errors are defined as follows:

$$
\begin{aligned}
S_\theta &\approx \left[B^2(\theta,\phi) + \Delta\beta^2(\theta,\phi,\varepsilon) + h^2\right]^{\frac{1}{2}} \ ; \quad \Delta\theta = 0 \\
S_\phi &= \phi \ ; \quad \Delta\theta = 0 \ .
\end{aligned}
\tag{B.3}
$$

31

ROTATION ANGLE Δθ = 0.°
σ₀ = 1.00°   h = 0.00°

VERTICAL ANGLE Φ

——— 0.°
— — 5.°
— —10.°
— · 20.°
— · — 30.°
········ 40.°
— ···· 50.°
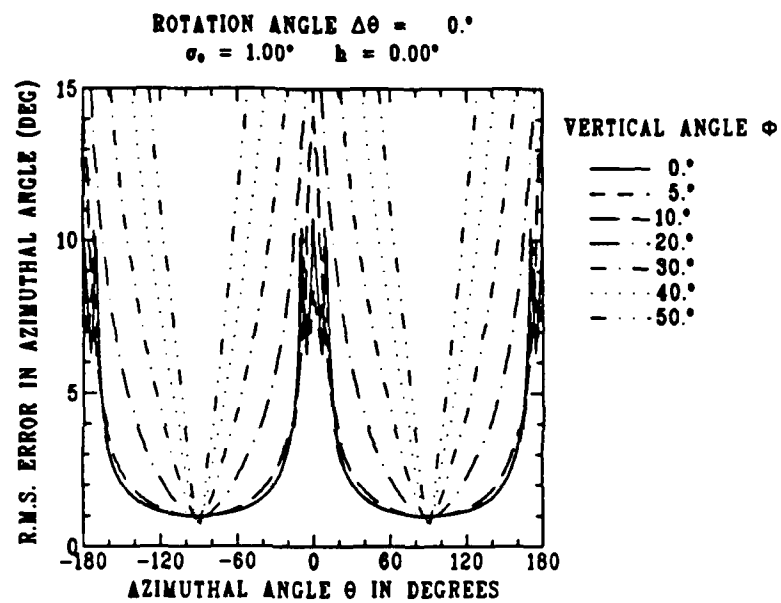
Figure B.1: Approximate r.m.s. error S_θ for the estimated azimuthal angle if the array is not rotated; $\sigma_0 = 1°$; $h = 0$.
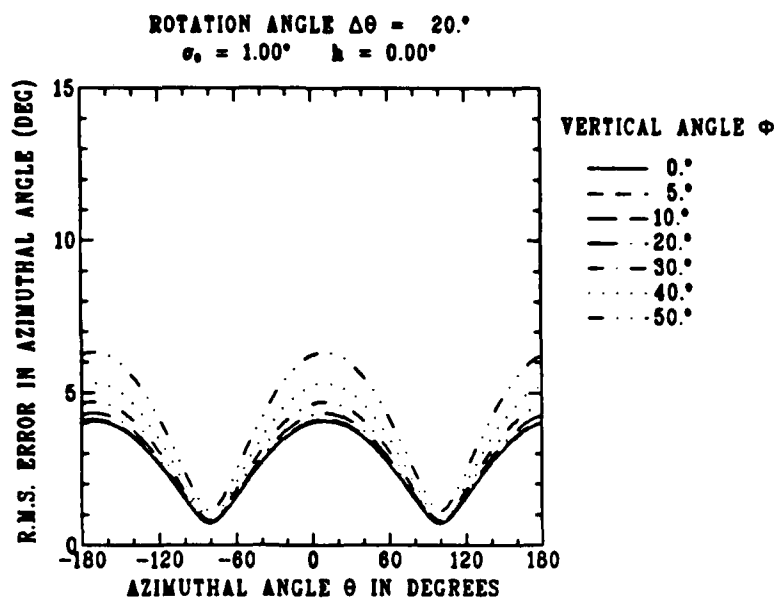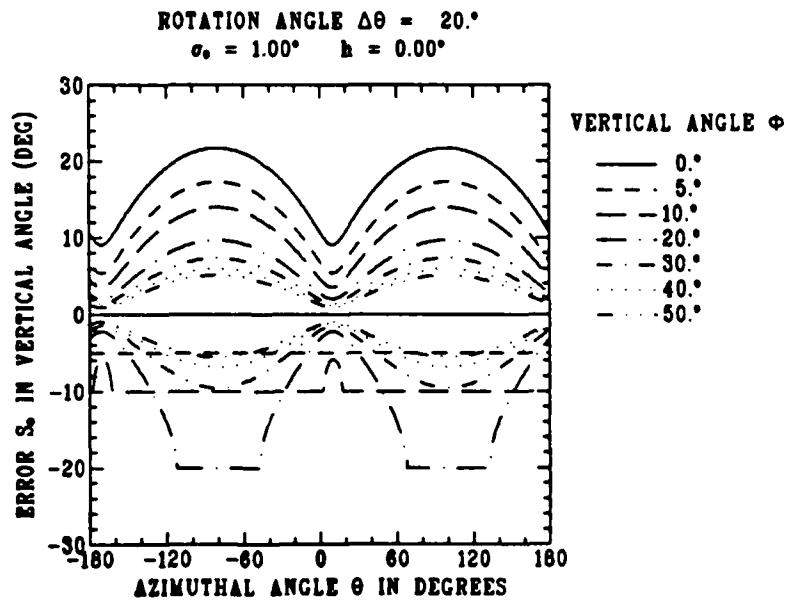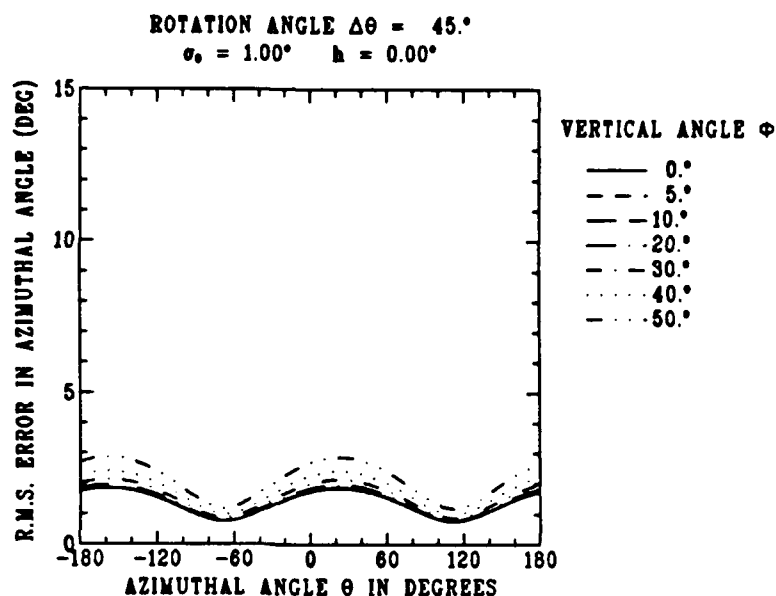
ROTATION ANGLE Δθ = 20.°
σ₀ = 1.00°   h = 0.00°

Figure B.2: Approximate r.m.s. error S_θ in azimuthal angle θ, as a function of θ and the vertical arrival angle ϕ, where the r.m.s. cosine error is $\sin\sigma_0$; $\sigma_0 = 1°$; rotation angle $\Delta\theta = 20°$; $h = 0$.
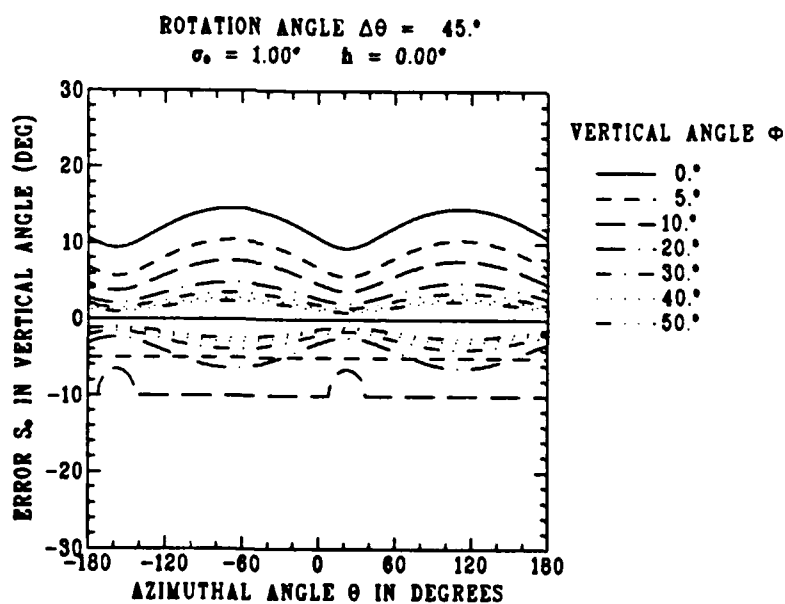
ROTATION ANGLE Δθ = 20.°
σ₀ = 1.00°   h = 0.00°

Figure B.3: Errors S_ϕ^+ and S_ϕ^- in vertical arrival angle ϕ, as a function of azimuthal angle θ, for several vertical arrival angles ϕ, where the r.m.s. cosine error is $\sin\sigma_0$; $\sigma_0 = 1°$; rotation angle $\Delta\theta = 20°$; $h = 0$.
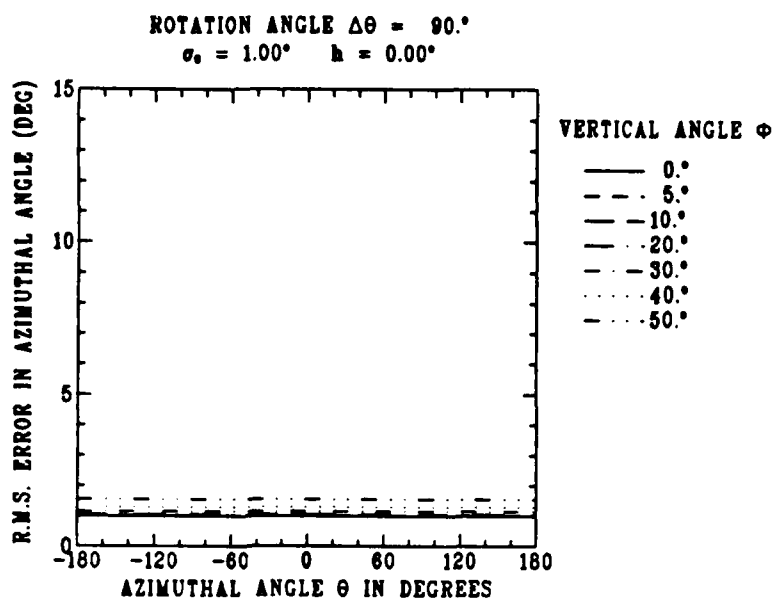
33

Figure B.4: Approximate r.m.s. error S_θ in azimuthal angle θ, as a function of θ and the vertical arrival angle ϕ, where the r.m.s. cosine error is $\sin \sigma_0$; $\sigma_0 = 1°$; rotation angle $\Delta\theta = 45°$; $h = 0$.
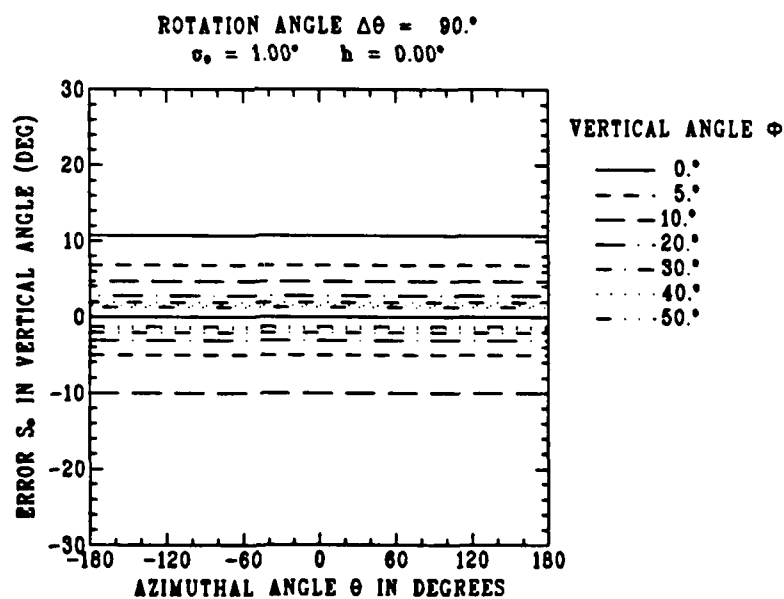

Figure B.5: Errors S_ϕ^+ and S_ϕ^- in vertical arrival angle ϕ, as a function of azimuthal angle θ, for several vertical arrival angles ϕ, where the r.m.s. cosine error is $\sin \sigma_0$; $\sigma_0 = 1°$; rotation angle $\Delta\theta = 45°$; $h = 0$.
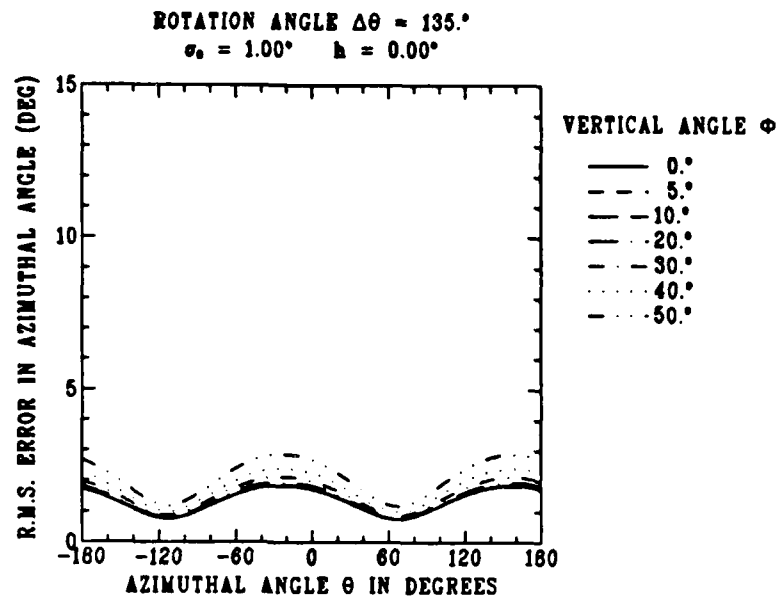
ROTATION ANGLE Δθ = 90.°
σ₀ = 1.00°   h = 0.00°

Figure B.6: Approximate r.m.s. error S_θ in azimuthal angle θ, as a function of θ and the vertical arrival angle ϕ, where the r.m.s. cosine error is $\sin \sigma_0$; $\sigma_0 = 1°$; rotation angle $\Delta\theta = 90°$; $h = 0$.
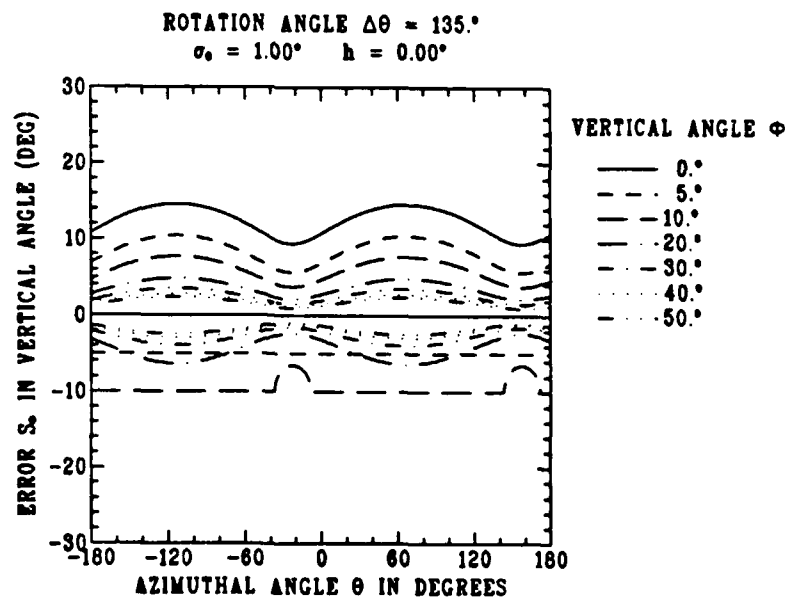

ROTATION ANGLE Δθ = 90.°
σ₀ = 1.00°   h = 0.00°

Figure B.7: Errors S_ϕ^+ and S_ϕ^- in vertical arrival angle ϕ, as a function of azimuthal angle θ, for several vertical arrival angles ϕ, where the r.m.s. cosine error is $\sin \sigma_0$; $\sigma_0 = 1°$; rotation angle $\Delta\theta = 90°$; $h = 0$.

35

ROTATION ANGLE Δθ = 135.°
σ₀ = 1.00°   h = 0.00°

R.M.S. ERROR IN AZIMUTHAL ANGLE (DEG)

VERTICAL ANGLE Φ
——— 0.°
— —. 5.°
— — 10.°
— · 20.°
— · — 30.°
········ 40.°
— ··· 50.°

AZIMUTHAL ANGLE θ IN DEGREES

Figure B.8: Approximate r.m.s. error S_θ in azimuthal angle θ, as a function of θ and the vertical arrival angle ϕ, where the r.m.s. cosine error is $\sin\sigma_0$; $\sigma_0 = 1°$; rotation angle $\Delta\theta = 135°$; $h = 0$.

ROTATION ANGLE Δθ = 135.°
σ₀ = 1.00°   h = 0.00°

ERROR S IN VERTICAL ANGLE (DEG)

VERTICAL ANGLE Φ
——— 0.°
— —. 5.°
— — 10.°
— · 20.°
— · — 30.°
········ 40.°
— ··· 50.°

AZIMUTHAL ANGLE θ IN DEGREES

Figure B.9: Errors S_ϕ^+ and S_ϕ^- in vertical arrival angle ϕ, as a function of azimuthal angle θ, for several vertical arrival angles ϕ, where the r.m.s. cosine error is $\sin\sigma_0$; $\sigma_0 = 1°$; rotation angle $\Delta\theta = 135°$; $h = 0$.

36

Appendix C   The Effect of Error in Rotation Angle

A number of graphs have been prepared to examine the sensitivity of the analytic solution to an error h in the rotation angle $\Delta\theta$. In all of the examples, $h = 1°$.

It is assumed in all of these cases that the observations $\cos\beta_1$ and $\cos\beta_2$ are exact, i.e. $\sigma_0 = 0°$. Four rotation angles 20°, 45°, 90°and 135°are considered. Several vertical arrival angles are examined. Figures C.2 to C.9 show the maximum errors resulting from a maximum error of 1°in the rotation angle. Figures C.11 to C.18 show the r.m.s. errors resulting from an r.m.s. error of 1°.

For purposes of comparison, figures C.1 and C.10 show the maximum error U_θ and the r.m.s. error S_θ for the case where the array is not rotated, and the vertical arrival angle is assumed to be zero.
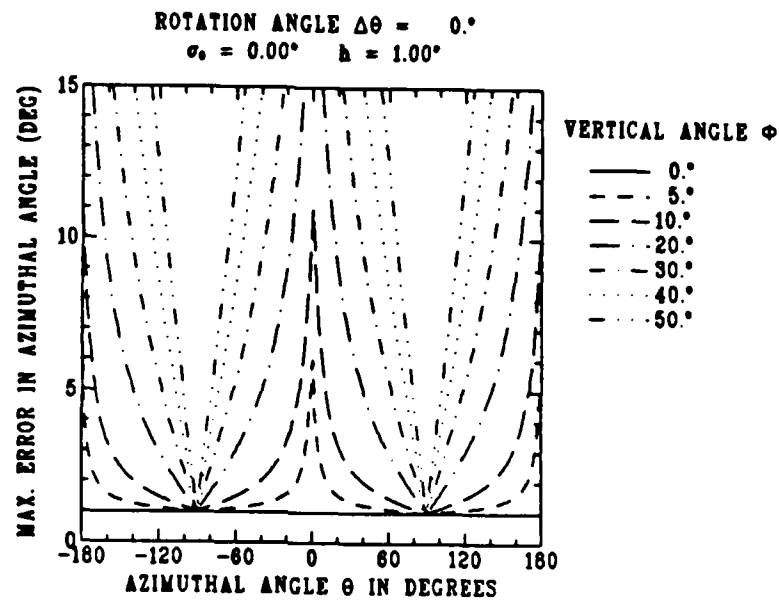
C.1 Maximum Errors Due to Error in Rotation Angle

Figure C.1: Bound U_θ on the maximum error in the estimated azimuthal angle if the array is not rotated; $\sigma_0 = 0°$; $h = 1°$.
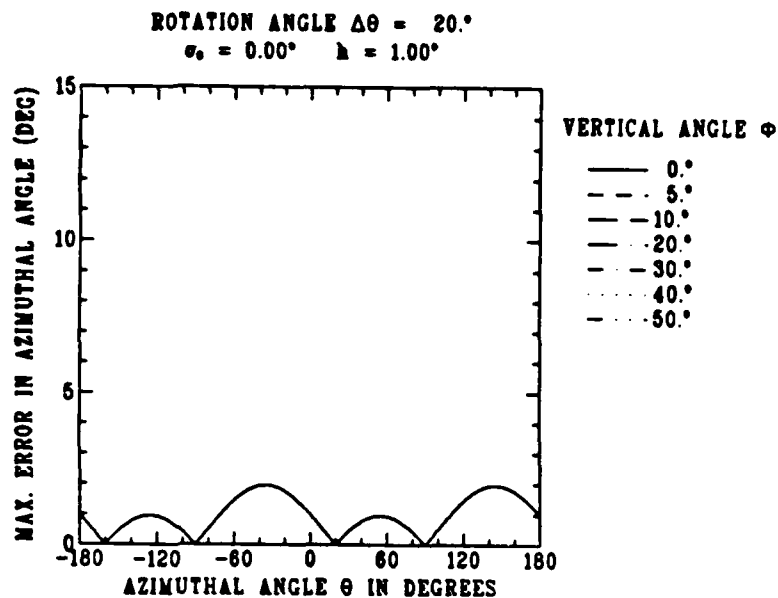
ROTATION ANGLE Δθ = 20.°
σ₀ = 0.00°   h = 1.00°

Figure C.2: Error bound U_θ on the estimated azimuthal angle θ, as a function of θ and the vertical arrival angle ϕ, where the maximum cosine error is $\sin\sigma_0$; $\sigma_0 = 0°$; rotation angle $\Delta\theta = 20°$; $h = 1°$.
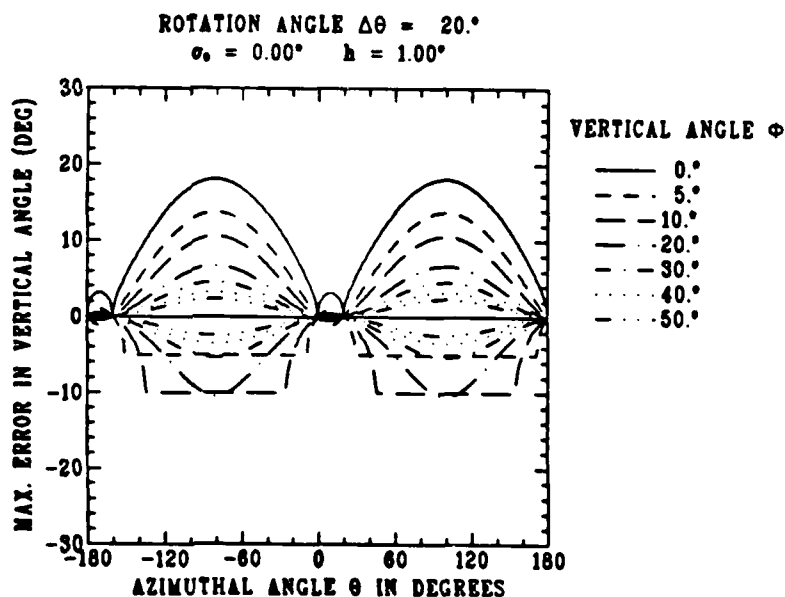
ROTATION ANGLE Δθ = 20.°
σ₀ = 0.00°   h = 1.00°

Figure C.3: Error bounds U_ϕ^+ and U_ϕ^- on the estimated vertical arrival angle ϕ, as a function of azimuthal angle θ, for several vertical arrival angles ϕ, where the maximum cosine error is $\sin\sigma_0$; $\sigma_0 = 0°$; rotation angle $\Delta\theta = 20°$; $h = 1°$.
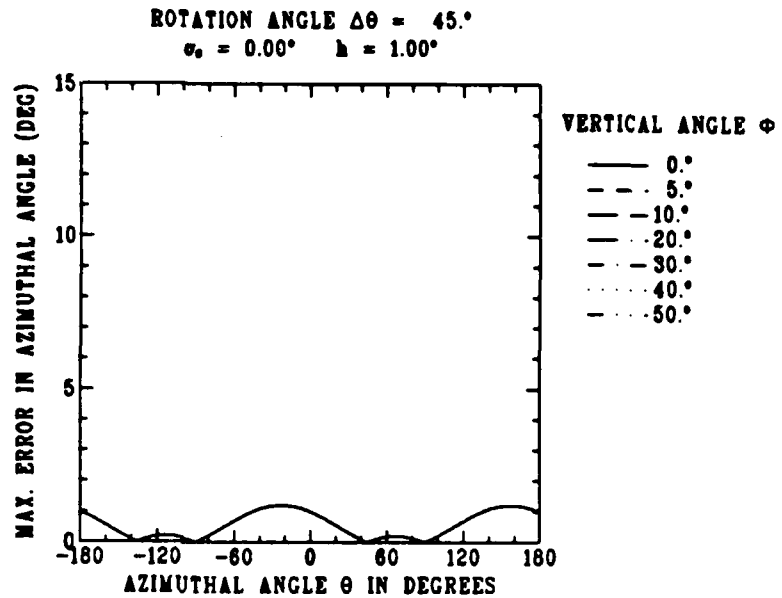
39

ROTATION ANGLE Δθ = 45.°
σ₀ = 0.00°   h = 1.00°

Figure C.4: Error bound U_θ on the estimated azimuthal angle θ, as a function of θ and the vertical arrival angle ϕ, where the maximum cosine error is $\sin \sigma_0$; $\sigma_0 = 0°$; rotation angle $\Delta\theta = 45°$; $h = 1°$.
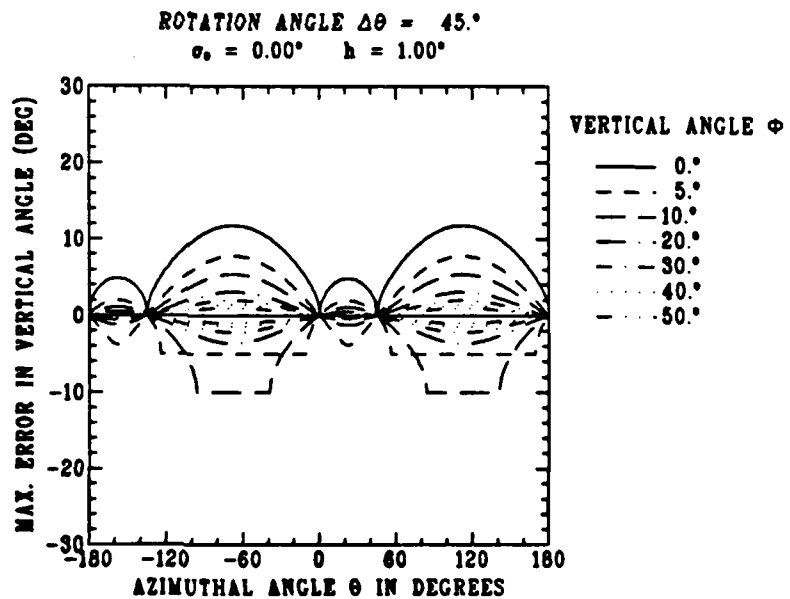

Figure C.5: Error bounds U_ϕ^+ and U_ϕ^- on the estimated vertical arrival angle ϕ, as a function of azimuthal angle θ, for several vertical arrival angles ϕ, where the maximum cosine error is $\sin \sigma_0$; $\sigma_0 = 0°$; rotation angle $\Delta\theta = 45°$; $h = 1°$.

ROTATION ANGLE Δθ = 90.°
σ₀ = 0.00° h = 1.00°

VERTICAL ANGLE Φ

——— 0.°
— — . 5.°
— —10.°
— . .20.°
— . —30.°
. . . . . 40.°
— . . . .50.°

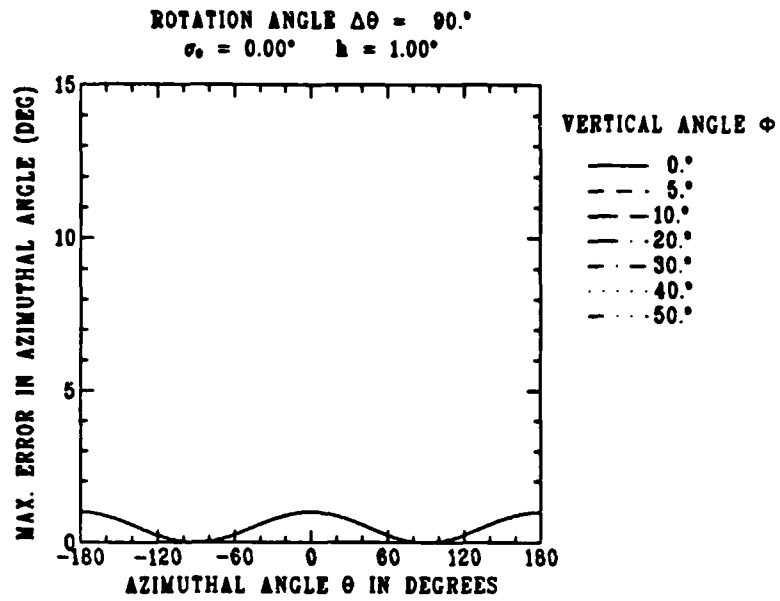MAX. ERROR IN AZIMUTHAL ANGLE (DEG)

AZIMUTHAL ANGLE θ IN DEGREES

Figure C.6: Error bound U_θ on the estimated azimuthal angle θ, as a function of θ and the vertical arrival angle ϕ, where the maximum cosine error is $\sin\sigma_0$; $\sigma_0 = 0°$; rotation angle $\Delta\theta = 90°$; $h = 1°$.

ROTATION ANGLE Δθ = 90.°
σ₀ = 0.00° h = 1.00°

VERTICAL ANGLE Φ

——— 0.°
— — . 5.°
— —10.°
— . .20.°
— . —30.°
. . . . . 40.°
— . . . .50.°

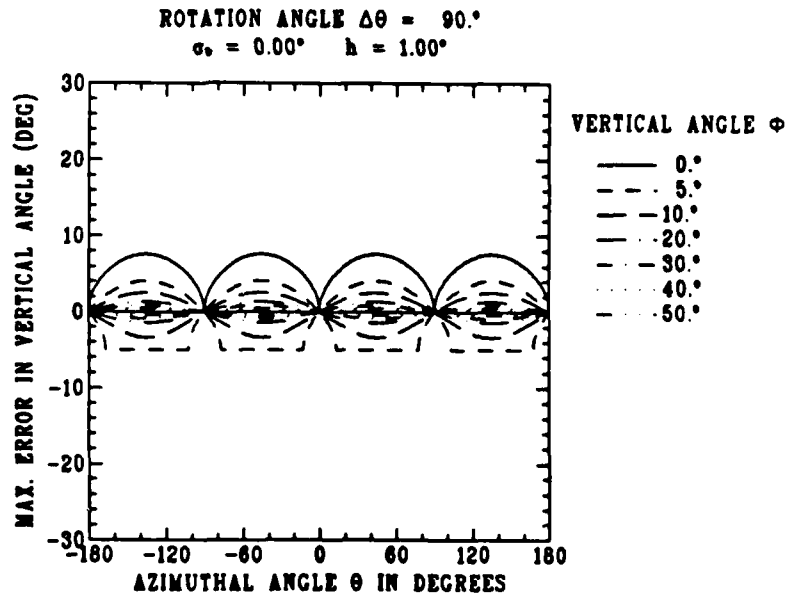MAX. ERROR IN VERTICAL ANGLE (DEG)

AZIMUTHAL ANGLE θ IN DEGREES

Figure C.7: Error bounds U_ϕ^+ and U_ϕ^- on the estimated vertical arrival angle ϕ, as a function of azimuthal angle θ, for several vertical arrival angles ϕ, where the maximum cosine error is $\sin\sigma_0$; $\sigma_0 = 0°$; rotation angle $\Delta\theta = 90°$; $h = 1°$.
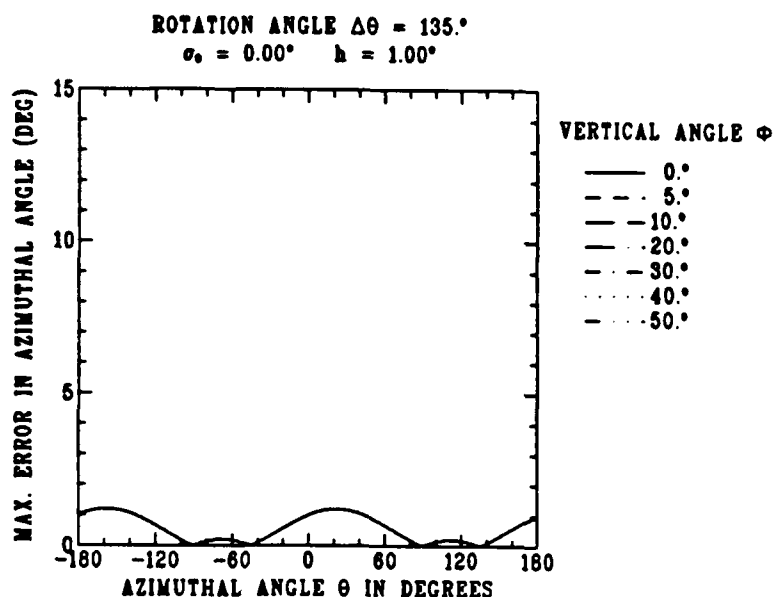
41

ROTATION ANGLE Δθ = 135.°

σ₀ = 0.00°   h = 1.00°

Figure C.8: Error bound U_θ on the estimated azimuthal angle θ, as a function of θ and the vertical arrival angle ϕ, where the maximum cosine error is $\sin\sigma_0$; $\sigma_0 = 0°$; rotation angle $\Delta\theta = 135°$; $h = 1°$.
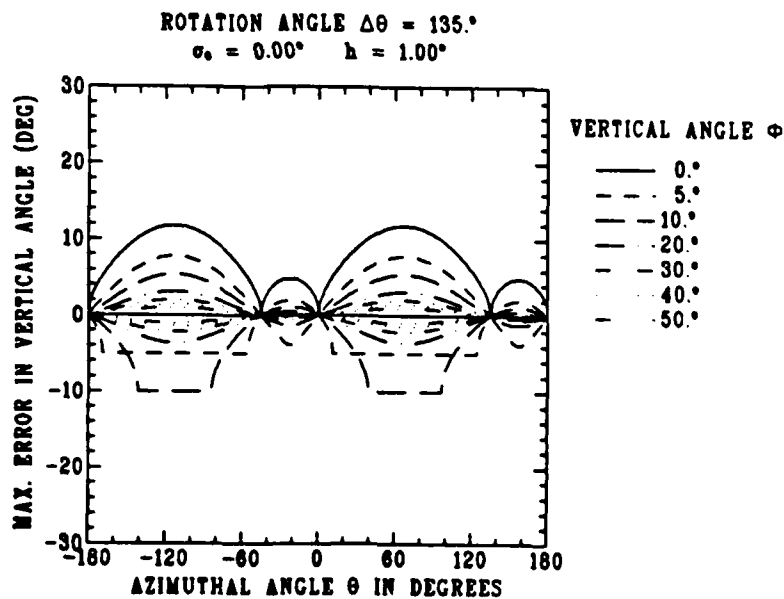
ROTATION ANGLE Δθ = 135.°

σ₀ = 0.00°   h = 1.00°

Figure C.9: Error bounds U_ϕ^+ and U_ϕ^- on the estimated vertical arrival angle ϕ, as a function of azimuthal angle θ, for several vertical arrival angles ϕ, where the maximum cosine error is $\sin\sigma_0$; $\sigma_0 = 0°$; rotation angle $\Delta\theta = 135°$; $h = 1°$.

42

C.2 R.M.S. Errors Due to Error in Rotation Angle

ROTATION ANGLE $\Delta\theta = 0.°$
$\sigma_0 = 0.00°$ $h = 1.00°$
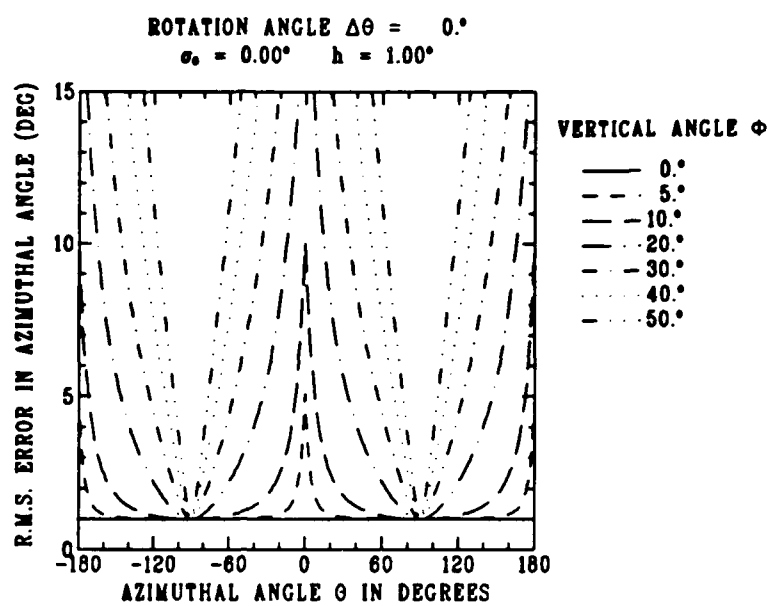

Figure C.10: Approximate r.m.s. error S_θ for the estimated azimuthal angle if the array is not rotated; $\sigma_0 = 0°$; $h = 1°$.
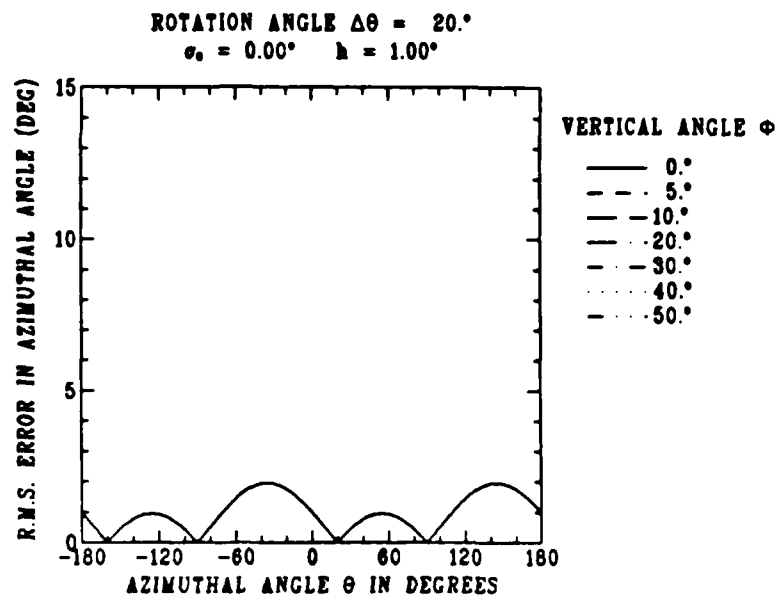
ROTATION ANGLE Δθ = 20.°
σ₀ = 0.00° h = 1.00°

Figure C.11: Approximate r.m.s. error S_θ in azimuthal angle θ, as a function of θ and the vertical arrival angle ϕ, where the r.m.s. cosine error is $\sin \sigma_0$; $\sigma_0 = 0°$; rotation angle $\Delta\theta = 20°$; $h = 1°$.
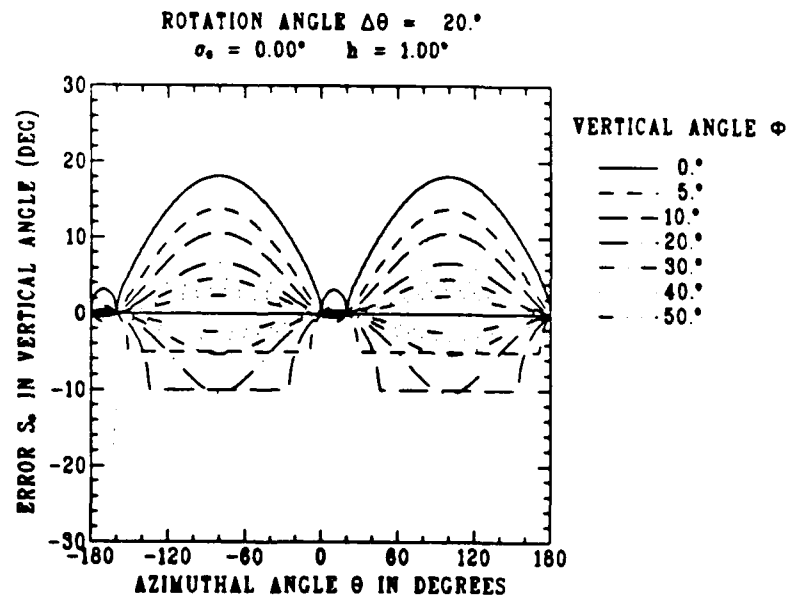
ROTATION ANGLE Δθ = 20.°
σ₀ = 0.00° h = 1.00°

Figure C.12: Errors S_ϕ^+ and S_ϕ^- in vertical arrival angle ϕ, as a function of azimuthal angle θ, for several vertical arrival angles ϕ, where the r.m.s. cosine error is $\sin \sigma_0$; $\sigma_0 = 0°$; rotation angle $\Delta\theta = 20°$; $h = 1°$.

44

ROTATION ANGLE Δθ = 45.°

σ₀ = 0.00°   h = 1.00°

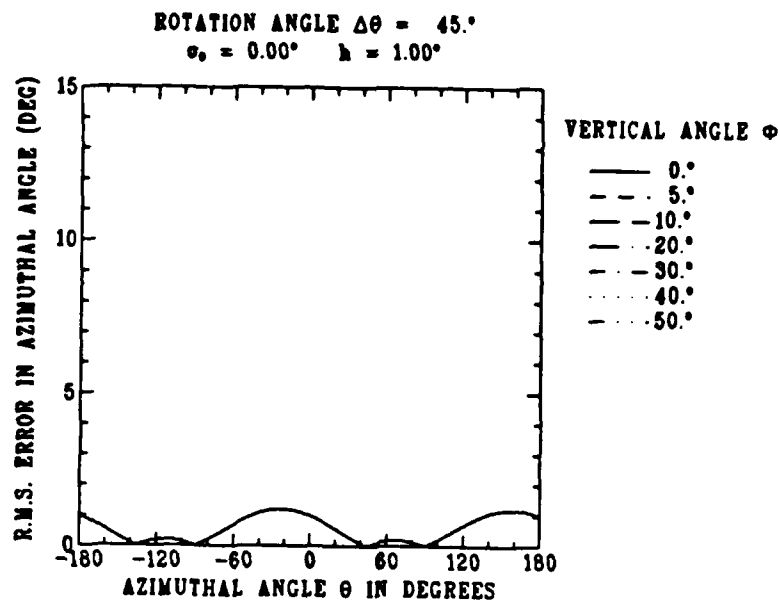

Figure C.13: Approximate r.m.s. error S_θ in azimuthal angle θ, as a function of θ and the vertical arrival angle ϕ, where the r.m.s. cosine error is $\sin\sigma_0$; $\sigma_0 = 0°$; rotation angle $\Delta\theta = 45°$; $h = 1°$.
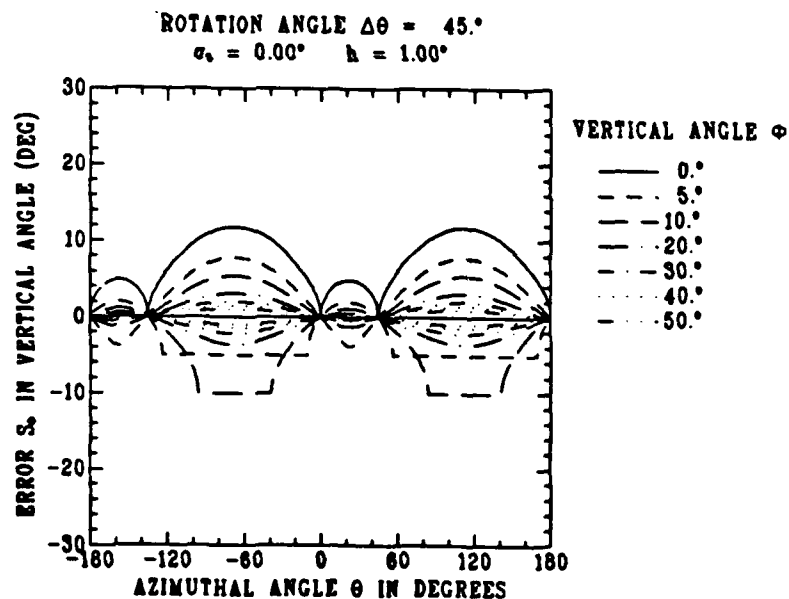
ROTATION ANGLE Δθ = 45.°

σ₀ = 0.00°   h = 1.00°

Figure C.14: Errors S_ϕ^+ and S_ϕ^- in vertical arrival angle ϕ, as a function of azimuthal angle θ, for several vertical arrival angles ϕ, where the r.m.s. cosine error is $\sin\sigma_0$; $\sigma_0 = 0°$; rotation angle $\Delta\theta = 45°$; $h = 1°$.

45

ROTATION ANGLE Δθ = 90.°
σ_φ = 0.00°   h = 1.00°

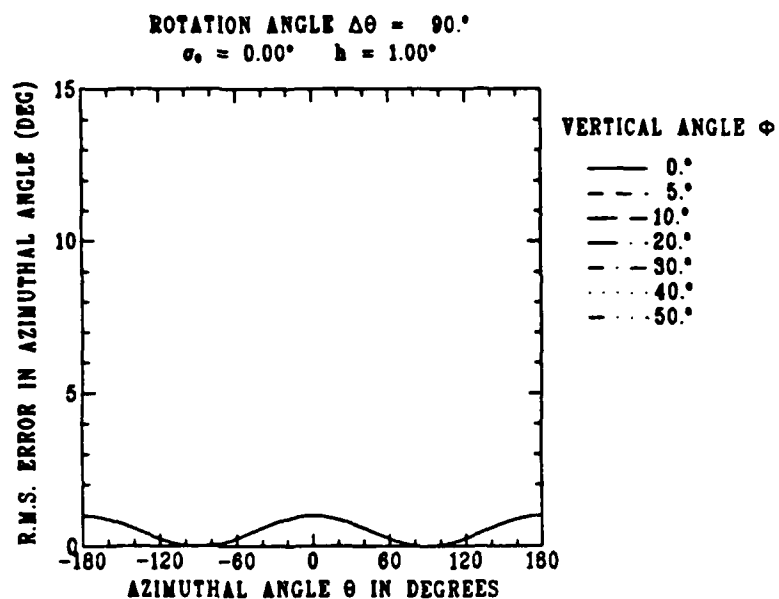

Figure C.15: Approximate r.m.s. error S_θ in azimuthal angle θ, as a function of θ and the vertical arrival angle ϕ, where the r.m.s. cosine error is $\sin\sigma_0$; $\sigma_0 = 0°$; rotation angle $\Delta\theta = 90°$; $h = 1°$.
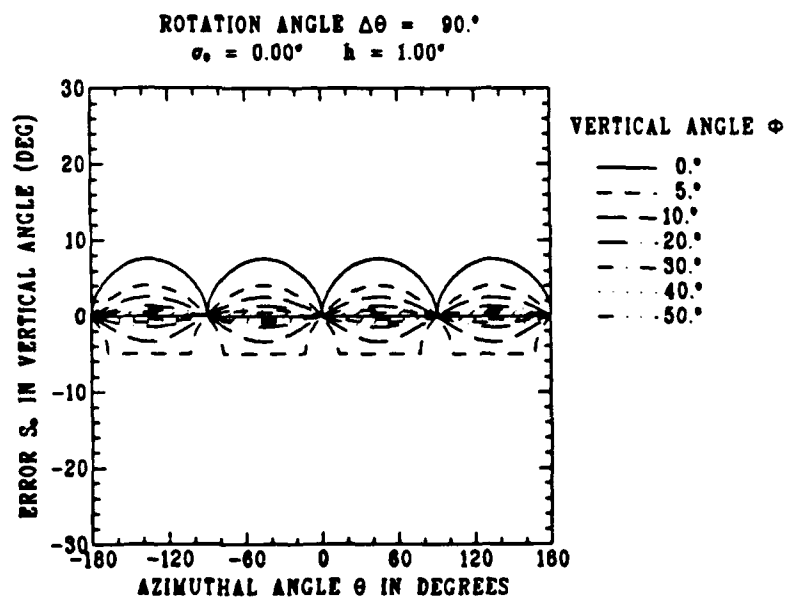
ROTATION ANGLE Δθ = 90.°
σ_φ = 0.00°   h = 1.00°

Figure C.16: Errors S_ϕ^+ and S_ϕ^- in vertical arrival angle ϕ, as a function of azimuthal angle θ, for several vertical arrival angles ϕ, where the r.m.s. cosine error is $\sin\sigma_0$; $\sigma_0 = 0°$; rotation angle $\Delta\theta = 90°$; $h = 1°$.
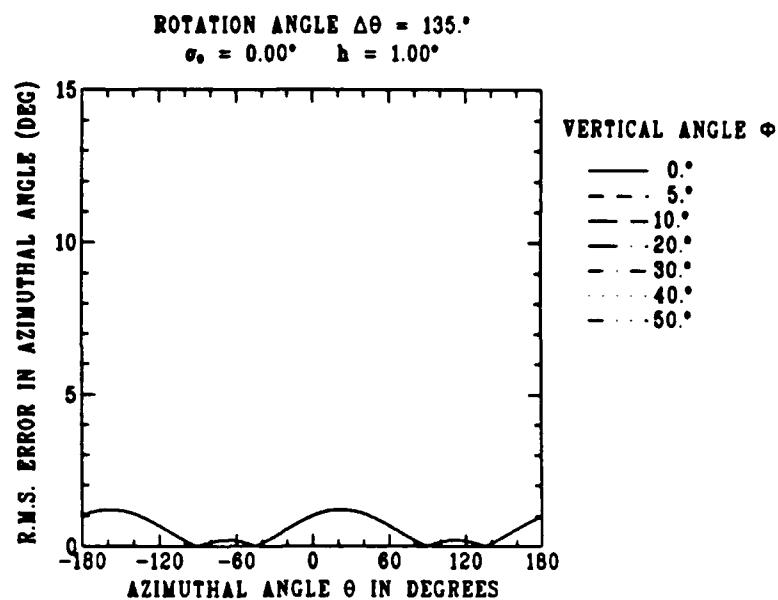
46

ROTATION ANGLE Δθ = 135.°

σ₀ = 0.00°   h = 1.00°

Figure C.17: Approximate r.m.s. error S_θ in azimuthal angle θ, as a function of θ and the vertical arrival angle ϕ, where the r.m.s. cosine error is $\sin\sigma_0$; $\sigma_0 = 0°$; rotation angle $\Delta\theta = 135°$; $h = 1°$.
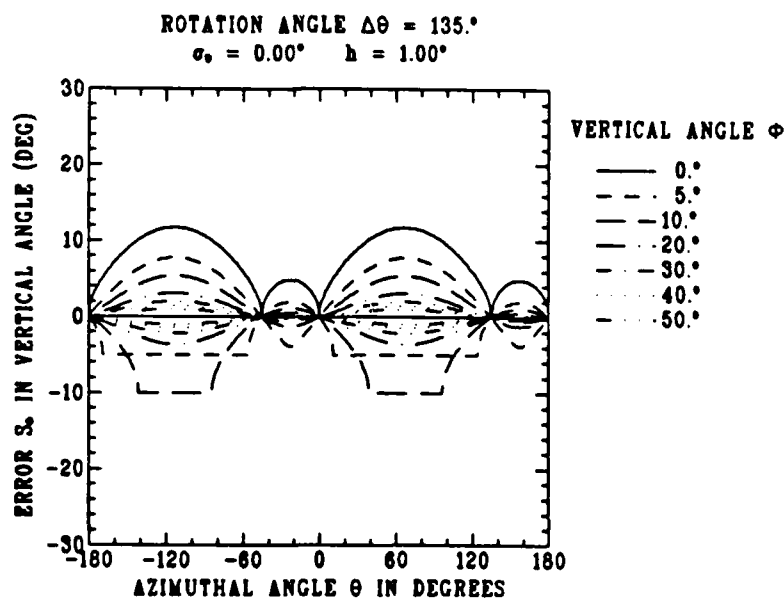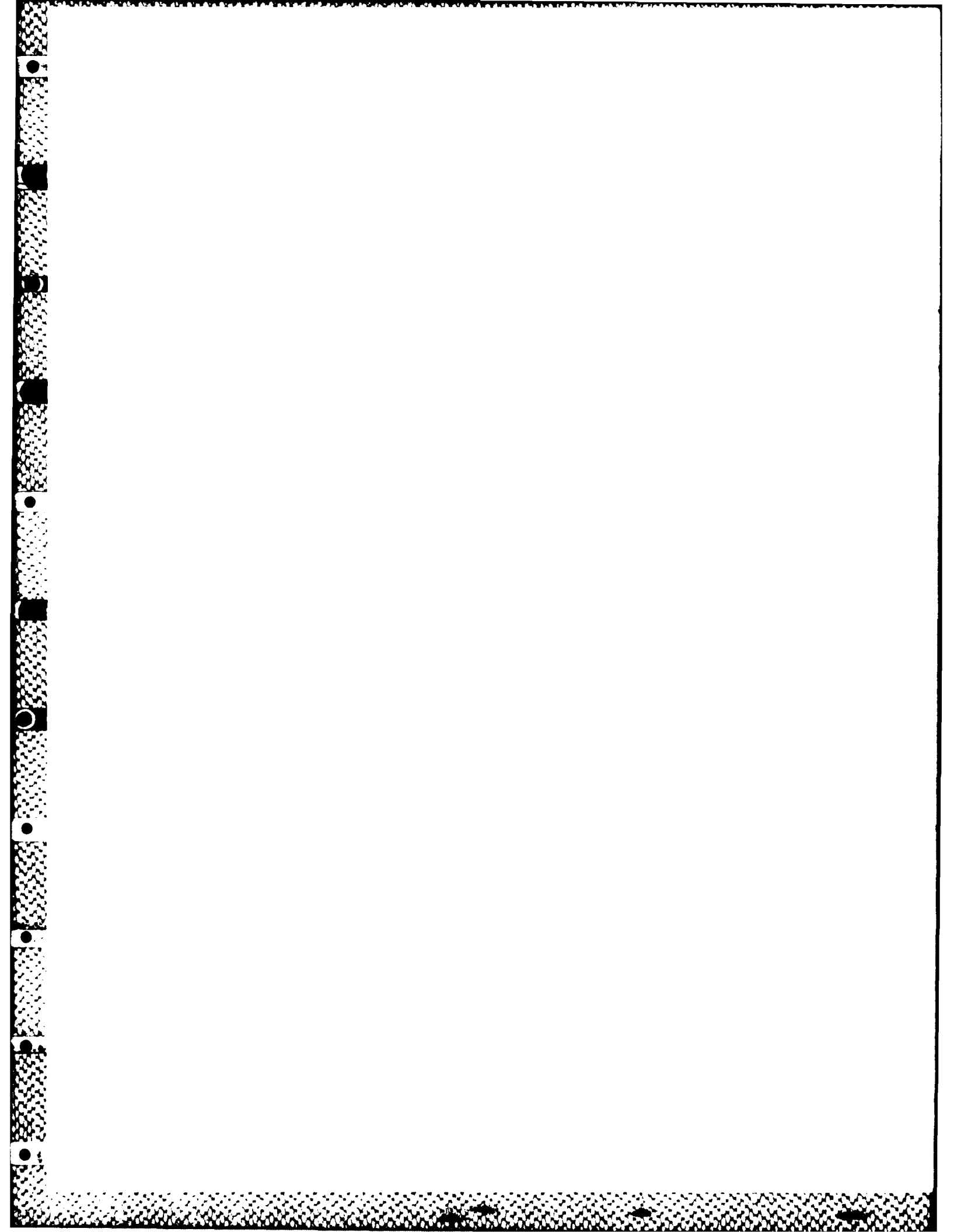

ROTATION ANGLE Δθ = 135.°

σ₀ = 0.00°   h = 1.00°

Figure C.18: Errors S_ϕ^+ and S_ϕ^- in vertical arrival angle ϕ, as a function of azimuthal angle θ, for several vertical arrival angles ϕ, where the r.m.s. cosine error is $\sin\sigma_0$; $\sigma_0 = 0°$; rotation angle $\Delta\theta = 135°$; $h = 1°$.

47

DOCUMENT CONTROL DATA

(Security classification of title, body of abstract and indexing annotation must be entered when the overall document is classified)

1. ORIGINATOR (the name and address of the organization preparing the document. Organizations for whom the document was prepared, e.g. Establishment sponsoring a contractor's report, or tasking agency, are entered in section 8.) Defence Research Establishment Atlantic	2. SECURITY CLASSIFICATION (overall security classification of the document including special warning terms if applicable) Unclassified

3. TITLE (the complete document title as indicated on the title page. Its classification should be indicated by the appropriate abbreviation (S,C,R or U) in parentheses after the title.)

ESTIMATION OF AZIMUTHAL AND VERTICAL ARRIVAL ANGLES AT A ROTATABLE HORIZONTAL LINE ARRAY (U)

4. AUTHORS (Last name, first name, middle initial. If military, show rank, e.g. Doe, Maj. John E.)

TRENHOLM, B. A. and THERIAULT, James A.

5. DATE OF PUBLICATION (month and year of publication of document) JULY 1987	6a. NO. OF PAGES (total containing information. Include Annexes, Appendices, etc.) 53	6b. NO. OF REFS (total cited in document) 2

7. DESCRIPTIVE NOTES (the category of the document, e.g. technical report, technical note or memorandum. If appropriate, enter the type of report, e.g. interim, progress, summary, annual or final. Give the inclusive dates when a specific reporting period is covered.)

DREA Report

8. SPONSORING ACTIVITY (the name of the department project office or laboratory sponsoring the research and development. Include the address.)

Defence Research Establishment Atlantic, P.O. Box 1012, Dartmouth, N.S. B2Y 3Z7

9a. PROJECT OR GRANT NO. (if appropriate, the applicable research and development project or grant number under which the document was written. Please specify whether project or grant) Research Project DRDA06	9b. CONTRACT NO. (if appropriate, the applicable number under which the document was written)

10a. ORIGINATOR'S DOCUMENT NUMBER (the official document number by which the document is identified by the originating activity. This number must be unique to this document.) DREA REPORT 87/101	10b. OTHER DOCUMENT NOS. (Any other numbers which may be assigned this document either by the originator or by the sponsor)

11. DOCUMENT AVAILABILITY (any limitations on further dissemination of the document, other than those imposed by security classification)

(X) Unlimited distribution
( ) Distribution limited to defence departments and defence contractors; further distribution only as approved
( ) Distribution limited to defence departments and Canadian defence contractors; further distribution only as approved
( ) Distribution limited to government departments and agencies; further distribution only as approved
( ) Distribution limited to defence departments; further distribution only as approved
( ) Other (please specify):

12. DOCUMENT ANNOUNCEMENT (any limitation to the bibliographic announcement of this document. This will normally correspond to the Document Availability (11). However, where further distribution (beyond the audience specified in 11) is possible, a wider announcement audience may be selected.)

Unlimited Distribution

13. ABSTRACT (a brief and factual summary of the document It may also appear elsewhere in the body of the document itself. It is highly desirable that the abstract of classified documents be unclassified. Each paragraph of the abstract shall begin with an indication of the security classification of the information in the paragraph (unless the document itself is unclassified) represented as (S), (C), (R), or (U). It is not necessary to include here abstracts in both official languages unless the text is bilingual)

A Horizontal Line Array (HLA) receiver is subject to left-right bearing ambiguity. It is also susceptible to bearing bias caused by non-zero vertical arrival angles. The true bearing angle and the vertical arrival angle may both be estimated if a second observation is made, with the HLA rotated to a neworientation. A closed-form solution is presented for the case of stationary source and receiver. For small observation errors, the resulting errors in the estimated angles can also be expressed in closed form.

14. KEYWORDS, DESCRIPTORS or IDENTIFIERS (technically meaningful terms or short phrases that characterize a document and could be helpful in cataloguing the document. They should be selected so that no security classification is required. Identifiers, such as equipment model designation, trade name, military project code name, geographic location may also be included. If possible, keywords should be selected from a published thesaurus e.g. Thesaurus of Engineering and Scientific Terms (TEST) and that thesaurus identified. If it is not possible to select indexing terms which are Unclassified, the classification of each should be indicated as with the title.)

Underwater Acoustics

Beamforming

Antenna

Ambiguity

Signal Processing

END

DATE
3-88
DTIC